JOC The Journal of Organic Chemistry

Article

pubs.acs.org/joc

Structural Basis of Duplex Thermodynamic Stability and Enhanced Nuclease Resistance of 5′-*C*-Methyl Pyrimidine-Modified Oligonucleotides

Alexander V. Kel′in,[†] Ivan Zlatev,[†] Joel Harp,[§] Muthusamy Jayaraman,[†] Anna Bisbe,[†] Jonathan O′Shea,[†] Nate Taneja,[†] Rajar M. Manoharan,[†] Saeed Khan,[‡] Klaus Charisse,[†] Martin A. Maier,[†] Martin Egli,[§] Kallanthottathil G. Rajeev,*[,†] and Muthiah Manoharan*[,†]

[†]Alnylam Pharmaceuticals, 300 Third Street, Cambridge, Massachusetts 02142, United States

[‡]Department of Chemistry and Biochemistry, University of California, Los Angeles, California 90095, United States

[§]Department of Biochemistry and Center for Structural Biology, Vanderbilt University, School of Medicine, Nashville, Tennessee 37232, United States

Supporting Information

ABSTRACT: Although judicious use of chemical modifications has contributed to the success of nucleic acid therapeutics, poor systemic stability remains a major hurdle. The introduction of functional groups around the phosphate backbone can enhance the nuclease resistance of oligonucleotides (ONs). Here, we report the synthesis of enantiomerically pure (*R*)- and (*S*)-5′-*C*-methyl (C5′-Me) substituted nucleosides and their incorporation into ONs. These modifications generally resulted in a decrease in thermal stability of oligonucleotide (ON) duplexes in a manner dependent on the stereoconfiguration at C5′ with greater destabilization characteristic of (*R*)-epimers. Enhanced stability against snake venom phosphodiesterase resulted from modification of the 3′-end of an ON with either (*R*)- or (*S*)-C5′-Me nucleotides. The (*S*)-isomers with different 2′-substituents provided greater resistance against 3′-exonucleases than the corresponding (*R*)-isomers. Crystal structure analyses of RNA octamers with (*R*)- or (*S*)-5′-*C*-methyl-2′-deoxy-2′-fluorouridine [(*R*)- or (*S*)-C5′-Me-2′-FU, respectively] revealed that the stereochemical orientation of the C5′-Me and the steric effects that emanate from the alkyl substitution are the dominant determinants of thermal stability and are likely molecular origins of resistance against nucleases. X-ray and NMR structural analyses showed that the (*S*)-C5′-Me epimers are spatially and structurally more similar to their natural 5′ nonmethylated counterparts than the corresponding (*R*)-epimers.

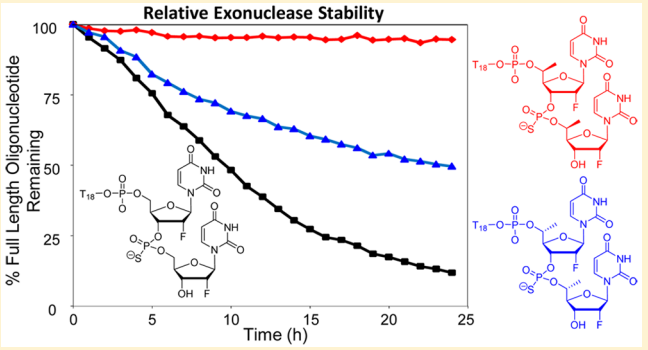

INTRODUCTION

RNA interference (RNAi) is a naturally occurring biological pathway of gene silencing that has been successfully harnessed to treat diseases using synthetic small interfering RNAs (siRNAs).[1−3] siRNAs formulated in lipid nanoparticles,[4] covalently conjugated to receptor-targeting ligand *N*-acetylgalactosamine (GalNAc),[5,6] and formulated in receptor targeting polymer-based delivery vehicles[7] are taken up by hepatocytes after systemic delivery and inhibit therapeutically relevant genes in humans. Optimal pharmacokinetic and pharmacodynamic properties of siRNA drugs require systemic stability. Work from our laboratory has demonstrated that chemical modifications can enhance systemic stability, which in turn results in more robust RNAi-mediated gene silencing *in vivo* compared to chemically less optimal siRNAs.[6] However, even these optimized siRNAs remain susceptible to nuclease degradation in tissues. Modifications that stabilize siRNAs against nucleases, the class of enzymes that degrades nucleic acids by cleaving internucleoside phosphodiester bonds,[8] are necessary.

The phosphate backbone of nucleic acids is the site of action for nucleases, and hence, many alterations of the internucleoside phosphodiester (PO) bond have been investigated. Several alternatives to the anionic PO backbone have been explored,[9] including charged or neutral phosphorus based designs such as phosphorothioates (with bridging and nonbridging sulfur atom),[10] phosphorodithioates,[11] methyl,[12] methylene,[13] and vinyl[14] phosphonates, phosphotriesters,[15] boranophosphates,[16] phosphoramidates,[17] phosphorodiamidates,[18] and nonphosphorus-based designs such as amides,[19] carbamates,[20] carbonates, oxyacetic esters and oxyacetamides,[21] formacetals,[22] and triazoles.[23] The phosphorothioate (PS) linkage with a non-

Received: November 12, 2015
Published: March 4, 2016

DOI: 10.1021/acs.joc.5b02375
J. Org. Chem. 2016, 81, 2261−2279

Scheme 1. Syntheses of 5′-*C*-Methyluridines[a]

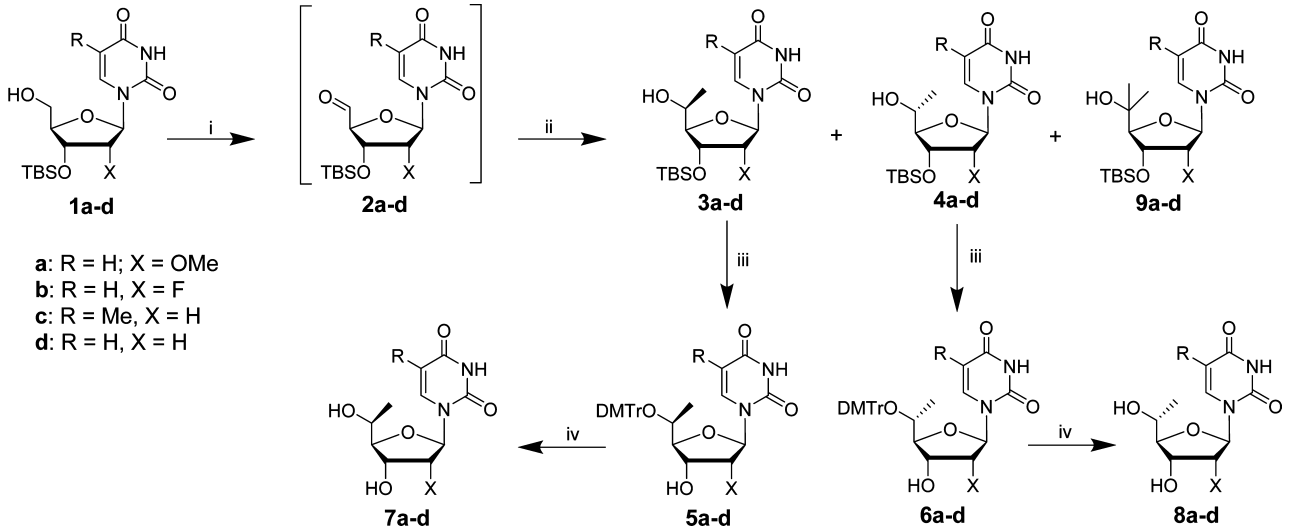

[a]Reagents and conditions: (i) Dess−Martin periodinane, DCM, 0 °C to r.t.; yields 93−99%, aldehyde content: 60−70%; (ii) CH_3MgBr, THF, −20 °C; 5′-(*S*)-isomer: 18−25%; (*R*)-isomer: 15−22% (based on **1a−d**); (iii) a. DMTr-Cl, $AgNO_3$/pyridine, b. TBAF/THF, 90−95%; (iv) HCl/EtOH, 91−94%.

bridging sulfur atom is found in most antisense therapeutics that are in clinical use.[24] The PS modification has also been explored in the context of siRNA; effects are position-dependent and multiple incorporations are counterproductive.[25,26]

The introduction of bulkier substituents around the phosphate backbone can enhance the nuclease resistance of ONs. For instance, alkyl substituents at various *C* positions of the sugar moiety modulate chemical, thermodynamic, and biological properties of both nucleosides[27−31] and ONs.[32−34] The methyl group is the simplest alkyl substituent that has been stereoselectively introduced in ribose and deoxyribose rings of nucleosides,[30] and *C*-methylated analogues have been evaluated as antitumor and antiviral agents,[28,29] in ribozymes,[35] and in antisense ONs.[32−34]

Substitution of the ribose hydrogens at C3′, C4′, C5′, or at both C5′ and C5″ positions with simple alkyls can exert a steric effect on the phosphodiester linkage between nucleotides. The alkyl substitution of C3′-H and C4′-H can significantly impact sugar conformation and may compromise the potency of siRNA.[36−38] Various alkyl substitutions at C5′ of the phosphate at the 5′-most position of single-stranded siRNA enhance nuclease resistance.[39] Here, we wanted to evaluate the impact of C5′-methylated nucleosides at internucleoside linkages in chemically modified RNA ONs.

In the present study, we report the synthesis and structural characterization of enantiomerically pure (*R*)- and (*S*)-5′-*C*-methyl (C5′-Me) substituted pyrimidine nucleosides with different 2′-substitutions including 2′-deoxy (2′-H), 2′-*O*-methyl (2′-OMe), and 2′-deoxy-2′-fluoro (2′-F). ONs substituted with these modified nucleosides were also studied. Both 2′-OMe and 2′-F ribo-substituents resulted in a C3′-*endo* sugar pucker, the ribose conformation observed in the A-type geometry of double-stranded siRNA.[40] We evaluated the impact of chirally pure C5′-Me ribonucleosides with different 2′-substitution on (i) sugar conformation using NMR and X-ray crystallography, (ii) thermal stability of 12-mer homo- and heteroduplexes containing a single C5′-Me incorporation, (iii) resistance against snake venom phosphodiesterase (SVPD), and (iv) duplex structure by X-ray crystallographic analysis of C5′-Me-modified octamer ONs and by studying models of RNAs bound at the active site of a 3′-exonuclease.

RESULT AND DISCUSSION

Synthesis of 5′-*C*-Methyl Nucleosides. Several approaches have been reported to synthesize 5′-*C*-alkyl nucleosides.[27−29,32,33,39,41−50] The addition of alkyl organomagnesium reagents to 5′-aldehydes of appropriately protected nucleosides affords both epimers in a single step; however, this method is complicated by the formation of insoluble magnesium residues and challenging separation of the epimers.[28,29,32,33,41−46] The use of magnesium or lithium alkyl cuprates or addition of cerium salts to the organomagnesium reagents did not increase yields or stereoselectivity.[45,51] Because of the difficulty of separation of the 5′ epimers, several studies utilized mixtures of (*R*)- and (*S*)-isomers.[28,29,33,44−46,51] In some cases, partial separation of the isomers was achieved using preparative TLC[43] or HPLC.[28,29] Separation of the 5′-epimers of 5′-*C*-alkyl-adenosine derivatives by selective enzymatic reaction with adenosine or adenylate deaminases, specific for the 5′-(*S*)-alkyl isomers, was also reported.[41,42]

Here, we describe an improved organomagnesium procedure for the synthesis of a variety of 5′-*C*-methyl pyrimidine nucleosides with different 2′-substituents and simple silica gel column chromatography and crystallization techniques for complete separation of the stereoisomeric products (Scheme 1). Dess−Martin oxidation[33,52] of 3′-*O*-TBS-protected nucleosides **1a−d** afforded unstable aldehydes **2a−d** that tend to form hydrates, cyclic products, and oligomers[41,44,52,53] and also can potentially undergo epimerization at the 4′-position.[43] The aldehydes **2a−d** constituted 60−70% of the crude mixtures as determined by ^{1}H NMR. Column chromatography purification was inefficient due to instability of aldehydes **2a−d**, so they were used in the next step without further purification. Attempts to use 2-iodoxybenzoic acid[54] or Swern-type protocols, including the Pfitzner−Moffatt modification,[43,44] yielded crude aldehydes of inferior purity.

DOI: 10.1021/acs.joc.5b02375
J. Org. Chem. 2016, 81, 2261−2279

Table 1. Estimated Percentages of C3′-*endo* Conformers for 2′-OMeU, 2′-FU, and dT and Their Corresponding (*R*)- and (*S*)-5′-*C*-Methyl Analogues in DMSO-d_6 Based on ^{1}H-NMR $^3J_{H\text{-}H}$ Coupling Constants

	substitution						
compound[a]	C2′	C3′	C5′[H(X)OH] X =	C5′-Me configuration	$^3J_{H1'\text{-}H2'}$ (Hz)	$^3J_{H3'\text{-}H4'}$ (Hz)	%N (C3′-*endo*)[b]
2′-OMeU	OCH_3	OH	H	NA	5.1	5.0	~50
1a	OCH_3	OTBS	H	NA	4.8		~50
3a	OCH_3	OTBS	CH_3	(*S*)	4.7		~50
4a	OCH_3	OTBS	CH_3	(*R*)	6.8	2.2	20−30
7a	OCH_3	OH	CH_3	(*S*)	5.0		~50
8a	OCH_3	OH	CH_3	(*R*)	6.4		~35
2′-FU	F	OH	H	NA	2.0		~80
1b	F	OTBS	H	NA	2.1	7.2	70−80
3b	F	OTBS	CH_3	(*S*)	2.3	6.8	70−80
4b	F	OTBS	CH_3	(*R*)	4.0	4.8	50−60
7b	F	OH	CH_3	(*S*)	2.2		~80
8b	F	OH	CH_3	(*R*)	3.6		~65
dT	H	OH	H	NA	7.3		~30
1c	H	OTBS	H	NA	7.8	2.8	20−30
3c	H	OTBS	CH_3	(*S*)	7.7	2.8	20−30
4c	H	OTBS	CH_3	(*R*)	8.9	1.5	10−15
7c	H	OH	CH_3	(*S*)	6.6		~30
8c	H	OH	CH_3	(*R*)	8.4		~15

[a]2′-OMeU: 2′-*O*-methyluridine; 2′-FU: 2′-deoxy-2′-fluorouridine, and dT: thymidine. [b]Calculated as an average of 10 × $^3J_{H3'\text{-}H4'}$ and 100−10 × $^3J_{H1'\text{-}H2'}$.

Slow addition of a solution of the crude aldehydes **2a−d** in anhydrous THF to a solution of excess methylmagnesium bromide (CH_3MgBr) in THF was performed, as opposed to the commonly used addition of alkyl organomagnesium to an aldehyde.[28,29,32,33,41−46] Reversing the mode of the addition prevented the formation of insoluble magnesium complexes and resulted in homogeneous reaction mixtures. About 5−15% of the aldehydes remained unreacted possibly due to hydration, intramolecular cyclization, or substrate oligomerization that led to partial "passivation" in the reaction.[44] Attempts to optimize the yields by protecting the N3 position of uridine were not successful. By testing reaction temperatures between −78 and 0 °C, we found that the cleanest reaction proceeded at around −20 °C bath temperature. The stereoisomeric mixtures of the resulting 5′-*C*-methyl nucleosides **3a−d** and **4a−d** were separated by silica gel column chromatography using eluents containing triethylamine (TEA). For the 2′-deoxy products **3c**, **3d**, **4c**, and **4d**, successive chromatographic purifications were performed in order to achieve complete separation of the epimers.

Although it was possible to separate 5′-methyl epimers on silica gel column in the presence of triethylamine, the individual epimers were contaminated with other inseparable impurities. It was found that the less polar (*S*)-isomers **3a−d** contained varying amounts of the 5′,5″-dimethyl derivatives **9a−d** (5−20%), whereas the more polar (*R*)-isomers **4a−d** could contain starting nucleosides **1a−d** (5−15%). The structural identities of the 5′,5″-dimethyl derivatives **9a−d** were confirmed by mass spectrometry analysis. As the tertiary 5′,5″-dimethyl nucleosides **9a−d** did not undergo 5′-tritylation in the presence of Ag(I), the (*S*)-isomers **3a−d** containing **9a−d** were treated with 4,4′-dimethoxytrityl chloride (DMTr-Cl) in the presence of silver nitrate and pyridine,[32] followed by 3′-*O*-desilylation, to afford **5a−d** (Scheme 1) easily separable from water-soluble desilylated **9a−d**. The crude (*R*)-isomers **4a−d** contaminated with **1a−d** were further purified either by crystallization or by successive chromatographic separation. In the case of **4a**, the reaction with DMTr-Cl in the absence of Ag(I) was performed. Under these conditions, only the primary hydroxyl in **1a**, that is present in the mixture reacted with DMTr-Cl, and the resulting tritylated nucleoside could be readily removed from **4a** by crystallization or chromatography. Pure (*R*)-isomers **4a−d** were then 5′-tritylated in the presence of Ag(I), followed by 3′-*O*-desilylation, to afford **6a−d** (Scheme 1).

In order to understand the impact of the *tert*-butyldimethylsilyl moiety on the 3′-oxygen on the ribosugar conformation of 5′-methylated pyrimidines, the corresponding unprotected nucleosides were also synthesized. A comparison of the sugar conformers of the 3′-*O*-TBS protected and unprotected nucleosides were estimated based on ^{1}H NMR $^3J_{H\text{-}H}$ coupling, and the results are summarized in Table 1. Fully deprotected nucleosides **7a−d** and **8a−d** were obtained by treatment of **5a−d** and **6a−d** with HCl in ethanol at ambient temperature.

2′-*O*-Methyluridines **5a** and **6a** were converted to the corresponding cytidine derivatives **10a** and **11a** in high yields using a *p*-nitrophenol-mediated procedure[55] (Scheme 2). A

Scheme 2. Syntheses of 5′-*C*-Methylcytidines[a]

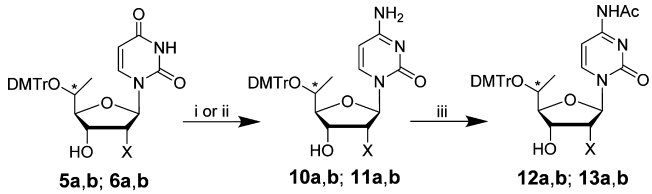

[a]Reagents and conditions: (i) **5a** and **6a**: a. TMS-Cl/NMP, CH_3CN; b. *p*-nitrophenol/trifluoroacetic anhydride, CH_3CN; c. NH_3/dioxane/H_2O, 81−85%; (ii) **5b** and **6b**: a. TMS-Cl/NMP, CH_3CN; 1,2,4-triazole/$POCl_3$/NMP, CH_3CN; b. NH_3/dioxane/H_2O, 64−65%; (iii) Ac_2O/DMF, r.t., 88−94%.

DOI: 10.1021/acs.joc.5b02375
J. Org. Chem. 2016, 81, 2261−2279

Scheme 3. Syntheses of Phosphoramidites and Solid Supports[a]

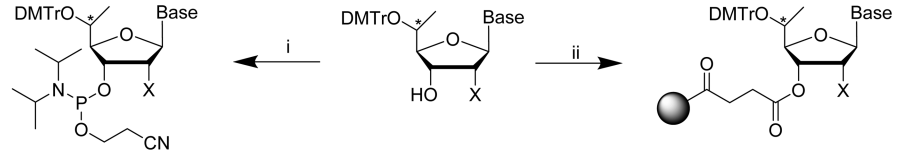

14a-d; **15a-d**; **16a,b**; **17a,b** **5a-d**; **6a-d**; **12a,b**; **13a,b** **18a,b**; **19a,b**; **20b**; **21b**

5a, **14a**, **18a**: 5'-*(S)*, Base = U, X = OMe
5b, **14b**, **18b**: 5'-*(S)*, Base = U, X = F
5c, **14c**: 5'-*(S)*, Base = T, X = H
5d, **14d**: 5'-*(S)*, Base = U, X = H
12a, **16a**: 5'-*(S)*, Base = C^{Ac}, X = OMe
12b, **16b, 20b**: 5'-*(S)*, Base = C^{Ac}, X = F

6a, 15a, 19a: 5'-*(R)*, Base = U, X = OMe
6b, **15b**, **19b**: 5'-*(R)*, Base = U, X = F
6c, **15c**: 5'-*(R)*, Base = T, X = H
6d, **15d**: 5'-*(R)*, Base = U, X = H
13a, **17a**: 5'-*(R)*, Base = C^{Ac}, X = OMe
13b, **17b, 21b**: 5'-*(R)*, Base = C^{Ac}, X = F

[a]Reagents and conditions: (i) 2-cyanoethyl *N*,*N*-diisopropylchlorophosphoramidite, DIEA, 85−95%; (ii) a. succinic anhydride, DMAP and b. HBTU, DIEA, lcaa CPG 500 Å, loading: 60−70 μmol/g.

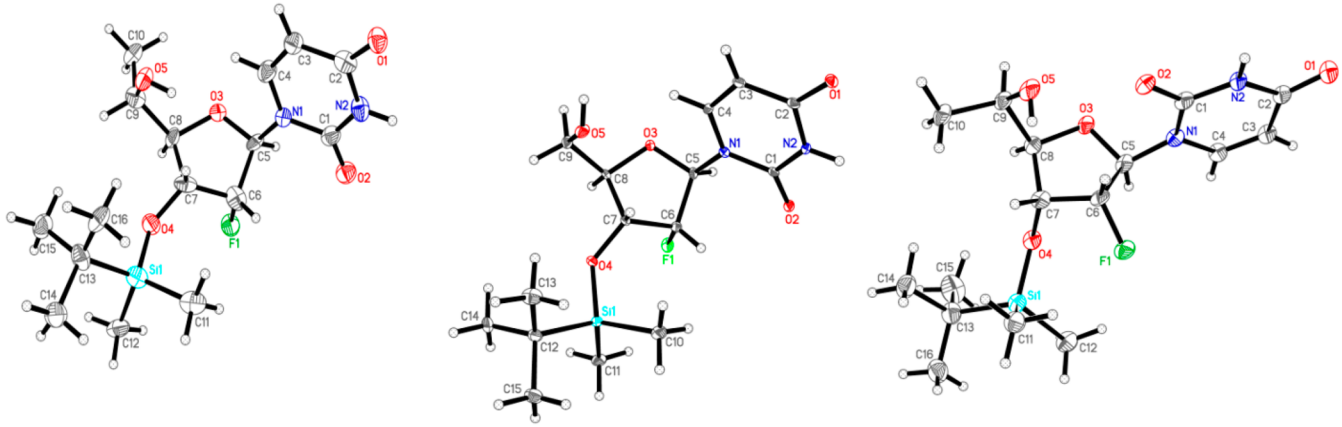

Figure 1. X-ray crystal structures of 3′-*O*-TBS-2′-FU (**1b**) and its 5′-*C*-methyl analogues **3b** and **4b**. The stereoconfigurations at C5′ for the isomers **3b** and **4b** are (*S*) and (*R*), respectively. The two stereoisomers adopt opposite C2′-C3′ sugar puckering and base orientations. The ellipsoid contour % probability level for all three structures is 50 at 100 K.

1,2,4-triazole-mediated protocol[56] that requires milder conditions for ammonolysis was used in an attempt to prevent base-induced defluorination of 2′-fluorouridine isomers **5b** and **6b** during the conversion to the corresponding cytidine nucleosides **10b** and **11b**. Moderate yields of **10b** and **11b** were obtained (64−65%) despite the milder conditions used. Treatment of the cytidine analogues **10a,b** and **11a,b** with acetic anhydride in DMF[56] afforded the corresponding N^4-acetylated nucleosides **12a,b** and **13a,b**.

Finally, 3′-*O*-phosphitylation of **5a−d**, **6a−d**, **12a**, **12b**, **13a**, and **13b** using 2-cyanoethyl *N*,*N*-diisopropylchlorophosphoramidite in the presence of diisopropylethylamine (DIEA) in DCM afforded the corresponding phosphoramidites **14a−d**, **15a−d**, **16a**, **16b**, **17a**, and **17b** (Scheme 3). Compounds **5a,b**, **6a,b**, **12a,b**, and **13a,b** were 3′-*O*-succinylated by treatment with succinic anhydride in the presence of DMAP in pyridine to obtain the corresponding hemisuccinates, which were subsequently coupled to a long chain amino alkyl (lcaa) functionalized controlled pore glass support (CPG) under HBTU-mediated amide coupling conditions to afford the desired solid supports **14a,b**, **15a,b**, **16a,b**, and **17a,b** with loading ranging between 60 and 70 μmol/g.

Configuration Assignment and Conformational Analysis. The absolute configurations of the C5′-Me stereocenters were unambiguously assigned using X-ray crystallography for compounds **3a−d** and **4a−d** bearing a 3′-*O*-TBS group (Figure 1 and the Supporting Information, Figure S3). The X-ray crystal structure of the (*R*)-isomer **4b** exhibited a C2′-*endo* (*South*) sugar pucker with *syn* base orientation, whereas the (*S*)-isomer **3b** had a C3′-*endo* (*North*) conformation and an *anti* base orientation. When the X-ray crystal structures of the two C5′-Me isomers were compared with that of the parent 2′-deoxy-2′-fluorouridine (2′-FU, **1b**, Figure 1), it was apparent that the conformation of the (*S*)-isomer **3b** was analogous to that of the parent nucleoside **1b**, whereas the corresponding (*R*)-isomer preferentially adopted the opposite C2′-*endo* sugar pucker and *syn* base orientation. The X-ray structures for the (*S*)-C5′-Me-3′-*O*-TBS-2′-OMeU (**3a**) and (*R*)-C5′-Me-3′-*O*-TBS-dU (**4d**) nucleosides could not be resolved.

To understand the impact of 2′-substitutions, we examined the X-ray crystal structures of the stereoisomers of 5′-*C*-methylated 2′-*O*-methyluridine (2′-OMeU), 2′-deoxyuridine (dU), and 2′-deoxythymidine (dT), all containing the 3′-*O*-TBS sugar protection (Supporting Information, Figure S3). In the crystal structure of the (*R*)-C5′-Me-3′-*O*-TBS-2′-OMeU

DOI: 10.1021/acs.joc.5b02375
J. Org. Chem. 2016, 81, 2261−2279

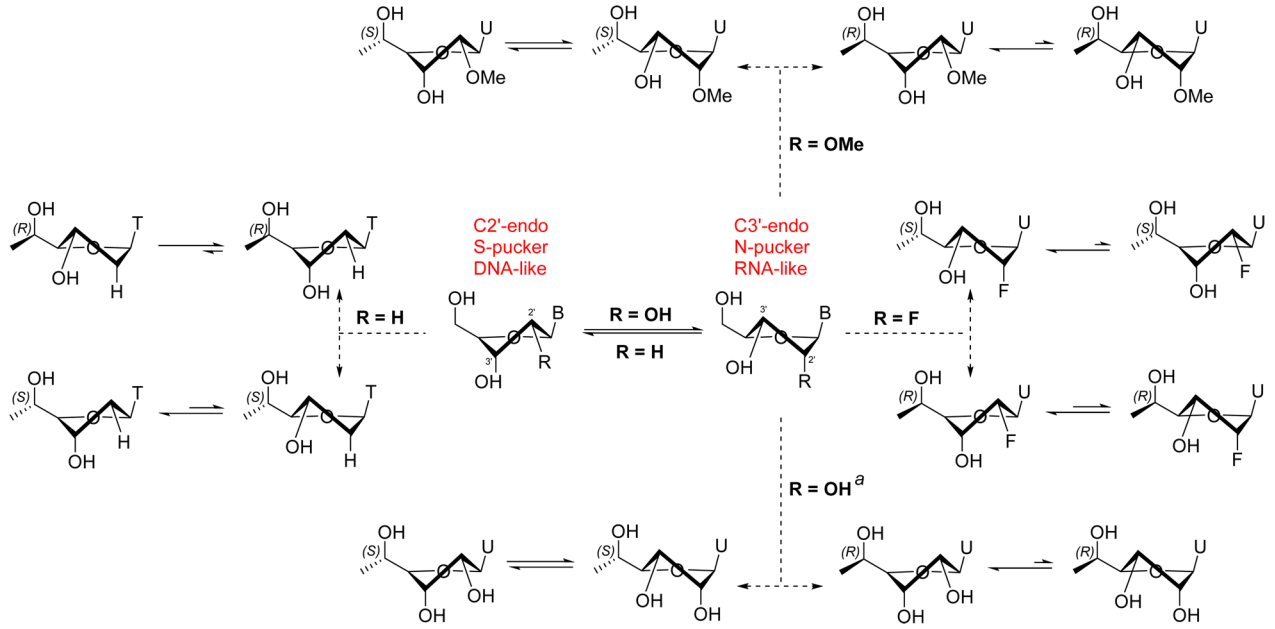

Figure 2. Conformational analysis of various 5′-*C*-methyl nucleosides and their stereoisomers based on the data from Table 1. [a]: Data from ref 31.

nucleoside **4a**, a C2′-*endo* sugar puckering with *syn* base orientation was observed, analogous to that of the (*R*)-isomer of C5′-Me-2′-FU **4b** (Figure 1). Interestingly, in the case of 5′-*C*-methyl-3′-*O*-TBS-2′-deoxythymidine, sugar pucker and base orientation of the (*S*)- and (*R*)-5′-*C*-methyl stereoisomers **3c** and **4c** and 3′-OH-dT counterparts **7c** and **8c** were identical (Figure S3). Both (*R*)- and (*S*)-isomers of the 2′-deoxy series crystallized in the C2′-*endo* conformation with *anti* base orientation, corroborating with X-ray crystal structural analysis data previously reported in the literature.[57] The crystal structures of 3′-*O*-TBS-2′-deoxyuridine (**1d**) and (*S*)-5′-*C*-methyl-3′-*O*-TBS-2′-deoxyuridine (**3d**), as well as the corresponding dT derivatives (**1c** and **3c**), all exhibited the C2′-*endo* sugar pucker and *anti* base orientation (Figure S3).

We explored the conformations of the 5′-*C*-methylated nucleosides with various 2′-substituents in solution using 1D and 2D NOESY ^{1}H NMR techniques. It is well established that the population of conformers on the pseudorotational cycle of the furanose ring of nucleosides, reflecting the values of the pseudorotational phase angle *P*, can be reliably predicted by the ^3J coupling constants in their 1D ^{1}H NMR spectra. A robust estimation of the *N* conformation (C3′-*endo*) can be obtained using the empirical equations established by Altona and Sundaralingam[58,59] and by Davies and Danyluk.[60] The $^3J_{H1'-H2'}$ and the $^3J_{H3'-H4'}$ coupling constants were determined directly from the first-order analysis of the 1D ^{1}H NMR spectra, where the approximate fraction of the C3′-*endo* conformer was determined as an average of the $10 \times {}^3J_{H3'-H4'}$ and $100-10 \times {}^3J_{H1'-H2'}$ values (Table 1)

The $^3J_{H-H}$ coupling constants (Table 1) obtained for the (*R*)- and (*S*)-isomers of 5′-*C*-methylated nucleosides clearly indicate that the stereochemistry of the 5′-*C*-methyl substitution in nucleosides affects the conformation of the furanose ring. The trend is conserved irrespective of 2′-substitutions (Figure 2). In RNA-like nucleosides (2′-FU and 2′-OMeU), the introduction of a 5′-*C*-methyl substitution in the (*S*)-configuration preserves the predominance of C3′-*endo* puckering (the conformation of sugars in an A-form helix), whereas the (*R*)-configuration shifts the pseudorotational equilibrium toward an increased population of C2′-*endo* sugar puckering. This observation corroborates the X-ray data on the (*R*)- and (*S*)-C5′-Me-2′-FU isomers (Figure 1). In the DNA-like 2′-deoxy series (dU and dT), the C2′-*endo* conformation observed in B-form DNA duplexes was predominant for both 5′-*C*-methyl isomers (Table 1). The (*S*)-5′-*C*-methyl isomers adopted the conformations of the nonmethylated parent nucleosides, whereas the (*R*)-5′-*C*-methyl conferred an even stronger C2′-*endo* pucker (Figure 2). This is in agreement with previously reported conformational studies on 5′-*C*-methyl deoxyribonucleoside analogues.[31]

Both, X-ray crystal structure and solution-phase NMR conformational analyses of the nucleosides indicate that the 5′-*C*-methyl substitution in the (*S*)-configuration preserves the sugar pucker conferred by the 5′ nonmodified parent nucleoside. In contrast, the 5′-*C*-methyl substitution in the (*R*)-configuration induced the C2′-*endo* ribose pucker in all cases, regardless of the ratio of preferred conformers present in the parent nucleosides. We concluded that the (*S*)-5′-*C*-methyl does not significantly alter the sugar puckering compared with that of the parent nucleosides, whereas the (*R*)-5′-*C*-methyl consistently confers a more pronounced DNA-like character on the resulting modified nucleosides.

We then analyzed the distribution of conformers around the exocyclic C4′−C5′ bond in order to determine the structural effect of the (*R*)- and (*S*)-*C*-methyl group at the C5′ of the modified nucleoside with respect to the corresponding parent nucleoside. Previously published structural studies of both (*S*)- and (*R*)-5′-*C*-methyl-2′-deoxythymidine using X-ray crystallography[57] and of 5′-(*R*)-*C*-methyluridine using NMR[47] demonstrated a C4′-C5′ conformation of *gauche*, *gauche* (*sc*+) with the hydroxyl group located above the furanose ring irrespective of the C5′-methyl stereochemistry.[47,57] In the case of 5′-*C*-methyl-2′-deoxythymidine, the observed *gauche*, *gauche* (*sc*+) conformation for both stereoisomers[57] differs from the *gauche*, *trans* (*ap*) conformation determined for the unmodified dT.[61]

The *gauche*, *gauche* (*sc*+) conformation was observed from the X-ray crystal structures (Figure 1 and Figure S3, Supporting Information) of all 2′-modified 5′-*C*-methyl nucleosides (Figure 3). Similarly, the 2D NOESY ^{1}H NMR analyses of the C4′-C5′

DOI: 10.1021/acs.joc.5b02375
J. Org. Chem. 2016, 81, 2261−2279

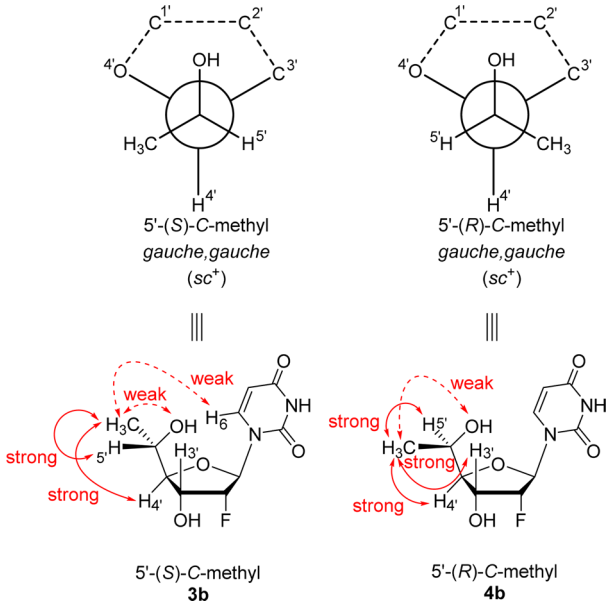

Figure 3. Newman projections of the prevalent rotamers of **3b** and **4b** with respect to the exocyclic C4′−C5′ bond of 5′-*C*-methyl nucleosides in (*R*) and (*S*) configurations as determined from X-ray crystal structures and from 2D NOESY ^{1}H NMR spectra.

conformations of (*S*)-C5′-Me-3′-*O*-TBS-2′-FU **3b** and (*R*)-C5′-Me-3′-*O*-TBS-2′-FU **4b** showed a prevalence for the *gauche*, *gauche* (*sc*+) conformation in solution based on the NOEs observed for the 5′-*C*-methyl group (Figure 3), in agreement with the crystal structure data on these isomers (Figure 1). The analysis supports the conclusion that 5′-*C*-methyl substitution confers a *gauche*, *gauche* (*sc*+) conformation around the exocyclic C4′−C5′ bond, for both 5′-stereoisomers regardless of the nature of the 2′-substitution on the nucleoside. The strong NOEs between H atoms of the methyl group and H-3′ for the (*R*)-isomers and the absence of the same for the (*S*)-isomers in the NOESY spectra, which also was reported for 5′-Me locked nucleic acids (LNA) derivatives based on crystal structural studies,[62] can be used to establish the configuration at the C5′ for other 5′-methylated pyrimidine nucleosides in the absence of X-ray structural data.

Effect of 5′-*C*-Methyl Modifications on Thermal Melting of Duplexes. In order to systematically evaluate the impact of structural perturbation exerted by the introduction of stereoisomerically pure (*R*)- and (*S*)-5′-*C*-methyl nucleotides, we performed studies centered on single incorporation of modified uridine derivatives into model sequences to understand the impact of 5′-*C*-methylation on stability against exonucleases, thermal melting, and duplex structure. The corresponding cytidines analogues were not included in these model studies.

The thermal melting temperatures (T_m) of DNA and RNA 12-mer homo- and heteroduplexes containing a single incorporation of both (*R*)- and (*S*)-5′-*C*-methylated uridine with H, F, and OMe 2′-ribosugar-substitutions, and (*R*)- and (*S*)-5′-*C*-methylthymdine were measured and compared with the corresponding unmodified duplexes (Table 2). The modifications were incorporated into one of the two strands at position 6 from the 5′ end. The modified strand was annealed with the complementary DNA or RNA strand to obtain the desired duplexes. The difference in T_m between the duplex with the modification and the corresponding unmodified homo- or heteroduplex (ΔT_m values) was used as a measure of the impact of each modification.

A single incorporation of RNA-like 2′-FU or 2′-OMeU into an RNA homoduplex had minimal effect on thermal stability of the duplex (Table 2, row IV), whereas incorporation of 2′-FU or 2′-OMeU into a DNA homoduplex resulted in duplex destabilization (Table 2, row I, ΔT_m −1.5 °C) relative to the unmodified control duplex.[63] A single incorporation of 2′-FU or 2′-OMeU into either the ribo- or the deoxyribo-strand of a 12-mer heteroduplex resulted in an increase in T_m compared to the unmodified heteroduplex (Table 1, rows II and III), which is presumably due to a propagation of the C3′-*endo* ribosugar conformation that results in a more A-like structure of the heteroduplex. Incorporation of dT into the RNA strand of the RNA/DNA duplex resulted in almost no change in thermal stability (Table 2, row III).

The effects of 5′-*C*-methylated 2′-FU, 2′-OMeU, and dT on thermal stability were dependent on C5′ stereochemistry and on the type of duplex. A single incorporation of 5′-*C*-methylated 2′-FU, 2′-OMeU, or dT into an RNA homoduplex was destabilizing, and the effect was more pronounced for the (*R*)- than for the (*S*)-isomers (Table 2, row IV). In a DNA homoduplex, a single incorporation of (*S*)-C5′-Me-2′-FU, which had a strong C3′-*endo* sugar pucker in solution and in the crystal structure as the monomer, slightly stabilized the

Table 2. Relative Melting Temperatures of ON Duplexes Modified with C5′-Methylated Nucleosides[a]

		ΔT_m/modification (°C)								
duplex[a]		**Q** = 2′-FU			**Q** = 2′-OMeU			**Q** = dT		
		C5′-H	(*S*)-C5′-CH_3	(*R*)-C5′-CH_3	C5′-H	(*S*)-C5′-CH_3	(*R*)-C5′-CH_3	C5′-H	(*S*)-C5′-CH_3	(*R*)-C5′-CH_3
I	DNA/DNA	−1.5	+0.3	−3.6	−1.7	+0.6	−2.3	0.0	−0.4	−0.6
II	DNA/RNA	+0.8	+2.3	−3.6	+1.3	+1.9	−2.0	0.0	−0.6	−4.0
III	RNA/DNA	+0.6	−0.6	−0.1	+0.5	−0.6	−1.2	−0.1	−2.9	−2.1
IV	RNA/RNA	+0.1	−0.9	−1.0	0.0	−0.9	−2.0		−3.2	−3.7
V	DNA/mmRNA	−1.5	+0.1	−7.2	−1.3	+0.6	−3.8	nd	nd	nd

[a]DNA/DNA: 5′-d(TACAG**Q**CTATGT)-3′/5′-d(ACATAGACTGTA)-3′; DNA/RNA: 5′-d(TACAG**Q**CTATGT)-3′/5′-r(ACAUAGACUGUA)-3′; RNA/DNA: 5′-r(UACAG**Q**CUAUGU)-3′/5′-d(ACATAGACTGTA)-3′; RNA/RNA: 5′-r(UACAG**Q**CUAUGU)-3′/5′-r(ACAUAGACUGUA)-3′; DNA/mmRNA: 5′-d(TACAG**Q**CTATGT)-3′/5′-r(ACAUAGGCUGUA)-3′, where **Q** indicates the chemical modifications within the ON. T_m values were measured in 1 × PBS buffer (pH 7.4) with a strand concentration of 2.5 μM; each T_m value is an average of two separate experiments. ΔT_m values were calculated by subtracting the T_m of the unmodified duplex from the T_m value of the corresponding modified duplex. T_m of the unmodified DNA/RNA: 42.6 °C; DNA/DNA: 42.9 °C; RNA/RNA: 53.6 °C; RNA/DNA: 39.8 °C; and DNA/mmRNA: 39.4 °C. DNA/mmRNA indicates DNA/RNA duplex with Q:G base pair, and nd stands for not determined.

DOI: 10.1021/acs.joc.5b02375
J. Org. Chem. 2016, 81, 2261−2279

Table 3. Half-lives ($T_{1/2}$) of 3′-End-Modified T_{18}-mer in the Presence of SVPD

	sequence (5′-3′)[a]	$T_{1/2}$ in the presence of SVPD (h)[b]								
		Q = 2′-FU			Q = 2′-OMeU			Q = dT		
		C5′-H	(*S*)-C5′-CH_3	(*R*)-C5′-CH_3	C5′-H	(*S*)-C5′-CH_3	(*R*)-C5′-CH_3	C5′-H	(*S*)-C5′-CH_3	(*R*)-C5′-CH_3
I	dT_{19}Q	nd	4.1	1.6	nd	1.9	1.3	nd	11.3	9.4
II	dT_{19}●Q	nd	>24	13.2	nd	24.0	4.6	2.5	13.5	8.6
III	dT_{18}QQ	0.3	19.1	18.5	0.2	19.0	11.0	nd	19.8	>24
IV	dT_{18}Q●Q	7.4	>24	23.2	11.4	18.8	18.6	2.5	>24	>24

[a]● indicates phosphorothioate (PS) linkage. [b]nd indicates not determined due to rapid nuclease digestion; >24 h indicates the 50% degradation was not observed. SVPD incubation time: 24 h at pH 7.4 and 37 °C. Full-length ON was quantified by IEX-HPLC (see the Supporting Information for more details).

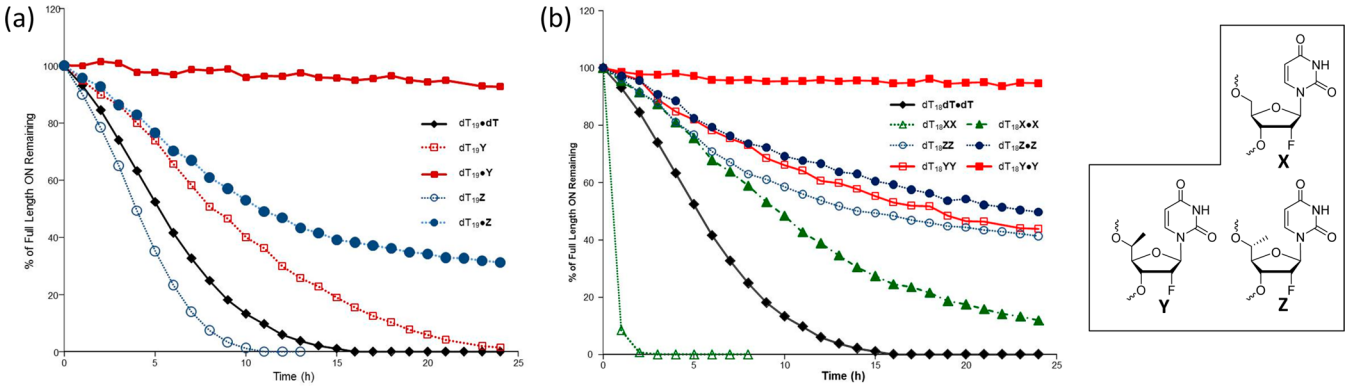

Figure 4. HPLC stability profiles of dT_{20} modified at the 3′ end with **X**, **Y**, or **Z** upon incubation with snake venom phosphodiesterase as a function of time. (a) Single incorporation with PO or PS linkage between dT and modified nucleosides and (b) double incorporation with PO and PS linkages between the two modified nucleosides. ● indicates PS linkage.

duplex (Table 2, row I). The DNA homoduplex stabilization effect was more pronounced for (*S*)-C5′-Me-2′-OMeU, which existed in a 1:1 C2′/C3′-*endo* equilibrium in solution, than for the (*R*)-isomer (Table 1 and Table 2, row I). Both (*R*)- and (*S*)-C5′-Me-dT slightly destabilized the DNA homoduplex.

Single incorporations of (*S*)-C5′-methyl-2′-FU or (*S*)-C5′-methyl-2′-OMeU into the DNA strand of the DNA/RNA heteroduplex enhanced the thermal stability of the duplex by about 2 °C. This thermal stabilization was significantly higher than the one afforded by the single incorporation of the corresponding 5′-unmodified 2′-FU or 2′-OMeU counterparts (Table 2, row II). Conversely, the (*R*)-C5′-methyl-2′-FU or (*R*)-C5′-methyl-2′-OMeU significantly destabilized the duplex when incorporated into the DNA strand of the DNA/RNA heteroduplex as opposed to the stabilization effect observed for the corresponding C5′-unmodified nucleotides (Table 2, row II). The $\Delta\Delta T_m$ values between (*S*)- and (*R*)-5′-*C*-methyl 2′-FU and (*S*)- and (*R*)-5′-*C*-methyl 2′-OMeU in a DNA/RNA heteroduplex context were +5.9 and +3.9 °C/modification, respectively (Table 2, row II), reflecting the effects of opposite sugar conformations conferred by each of the stereoisomers (Figure 2).

Incorporation of (*R*)- and (*S*)-5′-*C*-methyl 2′-FU or 2′-OMeU into the RNA strand of the RNA/DNA heteroduplex had little impact on T_m. The (*R*)-C5′-Me-2′-FU showed slight improvement in T_m over (*S*)-C5′-Me-2′-FU, whereas the (*R*)-C5′-Me-2′-OMeU destabilized the duplex compared to the corresponding (*S*)-isomer (Table 2, row III). Both (*R*)- and (*S*)-C5′-Me-dT destabilized the heteroduplexes. The destabilization caused by the (*R*)-C5′-Me-dT, relative to the corresponding (*S*)-isomer, was higher when the DNA strand of the heteroduplex was modified than when the RNA strand was modified, whereas the opposite trend was observed when the RNA strand was modified (Table 2, rows II and III).

Interestingly, when the modifications were placed in a DNA strand opposite to a mismatched complementary RNA strand (U-G wobble instead of U-A base pair, duplex V, Table 2), the discrimination between the (*S*)- and (*R*)-5′-*C*-methyl modifications were preserved or rather further enhanced, as the (*S*)-5′-*C*-methyl isomers conferred significant duplex stabilization compared to the (*R*)-5′-*C*-methyl isomers with respect to their C5′-H U-G wobble counterpart (Table 2, row V). The wobble base pairing in the duplex DNA/mmRNA caused 3.5 °C thermal destabilization to the heteroduplex. This T_m data plausibly indicating that strong conformational preference toward the *N* conformation, conferred by the (*S*)-5′-*C*-methyl modification, likely preserves thermal stability of DNA/RNA duplexes, even when placed opposite to a mismatched base pair.

Because of the *gauche*, *gauche* conformation around the exocyclic C4′−C5′ bond for both C5′-methyl isomers regardless of the 2′-modification (Figure 3), the γ dihedral angle is in the *sc*+ conformation in ONs. In the case of the (*R*)-isomers, the bulky 5′-methyl group is in an orientation that presumably negatively impacts hydration around the phosphate backbone,[64] which would cause duplex destabilization. The thermal melting data indicate that (i) the stereochemical configuration at C5′ is the major determinant of the homoduplex stability rather than the 2′-substitution and (ii) both the 5′-*C*-methyl stereochemistry and the 2′-substitution impact thermal stability in the case of heteroduplexes.

Effect of the 5′-*C*-Methyl Modification on Nuclease Stability. It has been reported that incorporation of a 5′-*C*-methylated residue at the 3′-end of a DNA[33] or LNA[62] ON

DOI: 10.1021/acs.joc.5b02375
J. Org. Chem. 2016, 81, 2261−2279

enhances stability against 3′-exonucleases. Stability of ONs against nucleases can also be achieved by introducing 2′-modifications or by replacing a PO with a PS linkage. To evaluate the 3′-exonuclease stability of combinations of C5′-methyl and 2′-modifications, a dT_{20} template sequence was modified at the 3′-end with either one or two modified nucleotides via PO or PS linkages (Table 3). ONs with two 2′-FU, 2′-OMeU, or dT residues with PO or PS linkages were used as the controls. ONs were incubated with snake venom phosphodiesterase (SVPD), and the half-life ($T_{1/2}$) of each modified ON was determined by HPLC-based quantification of the full-length ON as a function of time. The results are summarized in Table 3 and HPLC stability profiles are depicted in Figure 4.

The ONs with a single 2′-FU attached via either a PO or a PS linkage to the 3′-end of dT_{19} were degraded by the first time point upon incubation with SVPD (Table 3, rows I and II).[65] ONs modified with a single (*S*)- or (*R*)-5′-*C*-methyl-dT linked by a PO were considerably more stable with $T_{1/2}$ values of 11.3 and 9.4 h, respectively. The (*S*)-5′-*C*-methyl isomers of 2′-FU ($T_{1/2}$ = 4.1 h) and 2′-OMeU ($T_{1/2}$ = 1.9 h) linked through PO were more stable than the unmodified controls but, interestingly, were significantly less stable than the corresponding (*S*)-C5′-Me-dT analogue (Table 3, row I). The (*R*)-5′-*C*-methyl isomers of 2′-FU and 2′-OMeU linked by PO, with $T_{1/2}$ values of 1.6 and 1.3 h, respectively, also showed increased nuclease resistance compared to the corresponding non-methylated controls; however, they were less protective than the corresponding (*S*)-isomers. A similar trend was observed for (*S*)- and (*R*)-5′-*C*-Me-dT (Table 3, row I).

Replacing the PO linkage between the modified nucleotide and the dT_{19} with a PS linkage significantly improved the resistance against SVPD (Table 1, row II). The ON modified with (*S*)-C5′-Me-2′-FU linked through a PS was not degraded by SVPD during the 24 h incubation with the enzyme (Table 3, row II). The PS linkage similarly stabilized ONs modified with (*R*)-C5′-Me-2′-FU and with (*S*)- and (*R*)-C5′-Me-2′-OMeU. Interestingly, the impact of PS on stability was minimal when the 3′-terminal nucleotide was substituted with (*S*)- or (*R*)-5′-*C*-methyl dT (Table 3, X = dT, rows I and II).

Attachment of two 5′-*C*-methylated residues linked through either PO or PS resulted in a remarkable increase in resistance against SVPD-mediated degradation relative to singly modified ONs (Table 3, rows III and IV). Combinations of 5′-Me and 2′-substituents further protected the phosphodiester backbone against 3′-exonucleases than the PS linkage between their 5′-*C*-unmethylated counterparts. The level of protection was 5′-stereoconfiguration-dependent with the (*S*)-isomers providing more resistance to SVPD-mediated degradation than the (*R*)-isomers. These observations may not hold true with other exonucleases, and further evaluation is warranted in the context of single-stranded and double-stranded ONs to fully understand the stabilization potential of these modifications.

Crystal Structure of RNA Octamers Modified with (*R*)- or (*S*)-5′-*C*-Methyl-2′-Deoxy-2′-Fluorouridine. To gain a better understanding of the effects of (*S*)- and (*R*)-5′-*C*-methyl modification on the conformation of the RNA backbone in a duplex context, we carried out crystallization experiments with RNA duplexes containing a 5′-*C*-methylated 2′-deoxy-2′-fluoro nucleotide. Crystals were obtained for all three self-complementary duplexes with the sequence 5′-r[CGAA***X***UCG], where ***X*** is (*R*)-C5′-Me-2′-FU or (*S*)-C5′-Me-2′-FU, and 5′-r[CGAA-*d*TUCG], where dT is 2′-deoxythymidine. Structures for the duplexes were determined at resolutions of 1.8 Å (molecular replacement), 1.2 Å (bromine single wavelength anomalous dispersion, Br-SAD), and 1.99 Å (molecular replacement), respectively. The crystals of the (*R*)-C5′-Me-2′-FU-containing octamer and of the reference duplex contain two independent duplexes per asymmetric unit, and the (*S*)-C5′-Me-2′-FU-containing octamer crystal contains a single duplex per asymmetric unit. See the Supporting Information for details.

The 5′-*C*-methyl group of the (*R*)-C5′-Me-2′-FU-modified RNA duplex makes two intranucleotide contacts that are expected to negatively affect the thermodynamic stability. One is the 1···5 interaction between the methyl group and O3′ (avg. distance 3.04 Å), and the other is the 1···5 interaction between the methyl group and OP1 (avg. distance 3.19 Å) (Figure 5A; van der Waals radii: methyl 2.0 Å, oxygen 1.5 Å). All four strands with the (*R*)-C5′-Me-2′-FU residue adopt a conformation that is similar to that of the reference strand (Figure 5A,B). In terms of the structure-based interpretation of the thermodynamic consequences for pairing between an (*R*)-C5′-Me-2′-FU-modified RNA strand or an (*R*)-C5′-Me-2′-FU-modified DNA strand and the complementary RNA, it is evident that the two above contacts cannot be avoided in either the RNA or the DNA environments. The increased destabilization caused by an (*R*)-C5′-Me-2′-FU-modified DNA paired to RNA relative to the corresponding RNA duplex is most likely the result of the conformational heterogeneity as a consequence of insertion of a ribonucleotide (2′-F-RNA) between deoxyribonucleotides.

Simply using the structure of the (*R*)-C5′-Me-2′-FU-modified duplex as a template and flipping the configuration of the 5′-*C*-methyl group from *R* to *S* revealed two obvious, close contacts between that methyl group and neighboring atoms (Figure 5C). Both are of the internucleotide type. The first is between the methyl group and O3′ from the 5′-adjacent nucleotide. The second is between the methyl group and the 2′-hydroxyl group of the same 5′-adjacent nucleotide. The estimated distances are both around 2.50 Å, assuming that the backbone torsion angles (*sc-/ap/sc+/sc+/ap/sc-*; α to ζ) remain the same, independent of the configuration of the 5′-*C*-methyl group, and that the γ torsion angle does not undergo a significant rearrangement.

The crystal structure of the (*S*)-C5′-Me-2′-FU-modified duplex reveals how these close contacts are avoided in the context of the RNA backbone. In strand A, the 5′-*C*-methyl-modified U adopts an extended backbone conformation with α and γ torsion angles in the *ap* range and β assuming the standard *ap* conformation as well (Figure 5D). The sugar puckers of residues A4 and (*S*)-C5′-Me-2′-FU5 fall into the C3′-*endo* range. The distances between the methyl group and O3′ and O2′ from residue A4 are 3.19 and 6.11 Å, respectively. The distance between the O1P and 5′-*C*-methyl carbon atom is 3.49 Å. Thus, both the latter contact and the one between the methyl group and O3′ are longer than the corresponding average contacts in the (*R*)-5′-*C*-methyl-modified backbone (Figure 5A).

In the opposite strand (strand B), the (*S*)-5′-*C*-methyl-modified U displays a different conformation (Figure 5E). The backbone torsion angles fall into the *sc-/ap/sc+/sc+/ap/sc-* (α to ζ) ranges, and the sugars of both residues A4 and (*S*)-C5′-Me-2′-FU5 display the standard C3′-*endo* conformation. However, changes in the ζ and α torsion angles around the O3′−P and P−O5′ bonds, respectively, of the phosphate group of the 5′-*C*-methylated U5 result in longer distances between

DOI: 10.1021/acs.joc.5b02375
J. Org. Chem. 2016, 81, 2261−2279

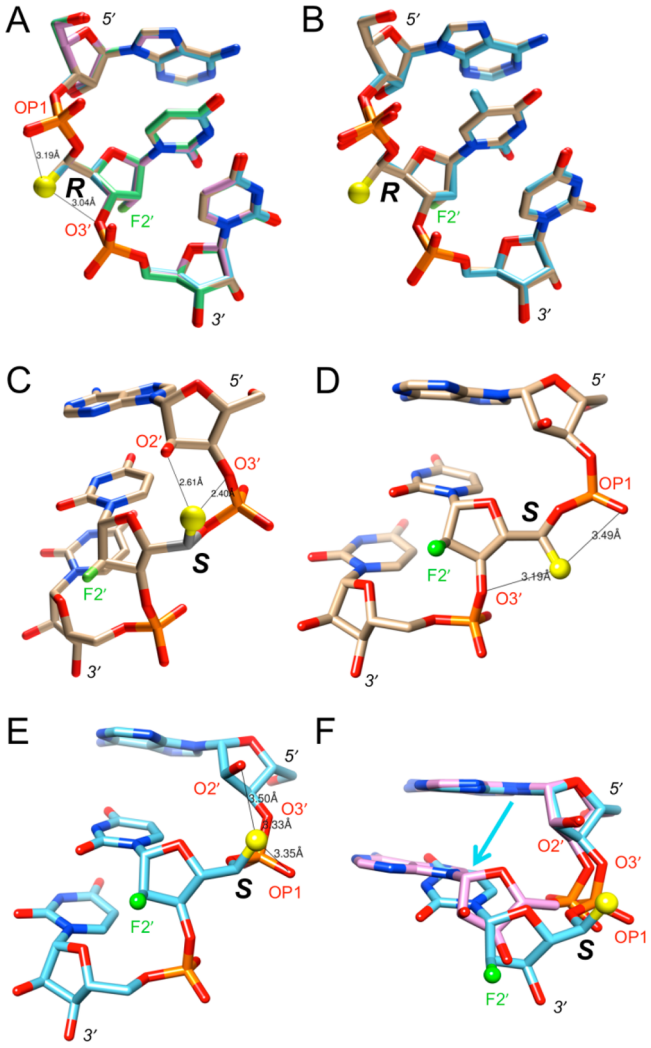

Figure 5. Structural properties of (*R*)-C5′-Me-2′-FU- and (*S*)-C5′-Me-2′-FU-modified RNA duplexes. (A) Superimposition of four trinucleotides 5′-A((*R*)-C5′-Me-2′-FU)U-3′ reveals nearly identical conformations of the four modified residues in the crystal lattice. Close contacts between the (*R*)-C5′-Me group (yellow sphere) and O1P and O3′ are indicated with thin solid lines, and average distances are given in Å. (B) Overlay between one of the trinucleotides 5′-A((*R*)-C5′-Me-2′-FU)U-3′ from the modified RNA (gray carbon atoms) and 5′-A(dT)U-3′ from the structure of the native RNA reference duplex with 2′-deoxythymidine (light blue carbon atoms). (C) Model of the (*S*)-C5′-Me-2′-FU-modified RNA constructed by flipping the conformation at C5′ from the crystal structure, with close contacts between the (*S*)-C5′-Me group (yellow sphere) and O2′ and O3′ from the preceding residue indicated with thin solid lines and average distances in Å. (D) Extended backbone conformation of (*S*)-C5′-Me-2′-FU in strand A of the modified duplex. (E) Conformation of (*S*)-C5′-Me-2′-FU in strand B. (F) Superimposition of the (A4)p((*S*)-C5′-Me-2′-FU5) (from panel E; cyan carbon atoms) and A3pA4 (lilac carbon atoms) base steps. The overlay demonstrates the different relative orientations of the 3′-nucleotides in the dimers, resulting in diminished stacking and a strong roll between bases as a consequence of 5′-*C*-methylation.

the methyl group and O3′ and O2′ (3.50 and 3.33 Å, respectively; Figure 5E) than those anticipated from the model constructed by simply flipping the methyl group from *R* to *S* (Figure 5C). The ζ angle in the crystal structure is −82° (−69° in the dT reference structure), and the α angle is −92° (−68° in the model). These angles push the (*S*)-5′-*C*-methyl group further from O2′ and O3′ than in the model; however, stacking at the (A4)p(C5′-Me-2′-FU5) base step is less favorable. This is evident from a superimposition of that step and the preceding A3pA4 step (Figure 5F; arrow). In the modified step, the uracil base is pushed away along with the 5′-*C*-methyl group and the conformational adjustment also creates a strong roll between adenine and uracil compared to the relative orientation of A3 and A4.

One of the potentially close contacts as a result of (*S*)-5′-*C*-methylation involves the 2′-hydroxyl group of the 5′-adjacent nucleotide readily explains the differential stabilities of (*S*)-C5′-Me-2′-FU incorporated into either RNA or DNA and paired opposite RNA. The lack of a 2′-OH at the 5′-neighboring nucleotide in the DNA context removes one of the steric clashes for (*S*)-C5′-Me-2′-FU (avoidance of the clash comes with an energetic penalty; Figure 5C–F). By comparison, (*R*)-C5′-Me-2′-FU cannot escape either close contact as both are intranucleotide (Figure 5A).

In addition to these steric complications, the (*R*)-configured 5′-*C*-methyl group—but not the (*S*)—is expected to interfere with conserved hydration patterns between adjacent phosphate groups in A-form duplexes.[64,66] Single water molecules bridge neighboring OP2 atoms in the major groove, and tandem water bridges connect adjacent OP1 atoms at the groove periphery. (*R*)-5′-*C*-methylation inserts a hydrophobic moiety into an otherwise polar hydrogen bonded region (Figure 6A). In contrast, the (*S*)-5′-*C*-methyl group is directed away from the water structure that surrounds the phosphate backbone (Figure 6B).

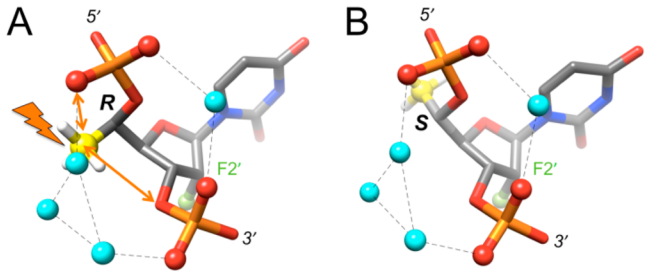

Figure 6. Consequences of the (A) (*R*)-C5′-Me-2′-FU and (B) (*S*)-C5′-Me-2′-FU modifications on hydration around the sugar-phosphate backbone. To build the models of the hydrated (*R*)-C5′-Me-2′-FU and (*S*)-C5′-Me-2′-FU nucleotides, water molecules (cyan spheres) from the crystal structure of an A-form duplex determined at 0.83 Å resolution[66] were fused with the crystal structures of an (*R*)-C5′-Me-2′-FU- and an (*S*)-C5′-Me-2′-FU-modified nucleotide. The (*R*)-C5′-Me group interferes with hydrogen bonding networks (dashed lines). Methyl carbon atoms are shown as yellow spheres.

Structural Basis of the Increased Nuclease Resistance Conferred by 5′-*C*-Methylation. Methylation at C5′ leads to markedly enhanced protection of ONs against degradation relative to the corresponding 5′-CH_2-2′-F RNA ONs, as demonstrated by the exonuclease assay (Figure 4, Table 3). Our crystallographic analysis suggests that the protection has stereoelectronic and steric origins. The presence of the 5′-*C*-methyl group likely reduces the reactivity of the phosphate group toward a nucleophile (e.g., a hydroxide ion or a deprotonated 2′-hydroxyl group at the active site of an exonuclease[67] or adjacent to the scissile bond in a ribozyme,[68] respectively).

DOI: 10.1021/acs.joc.5b02375
J. Org. Chem. 2016, 81, 2261−2279

Addition of a methyl group at the 5′-position in the structural model of a 3′-5′ exonuclease (*E. coli DNA polymerase I Klenow fragment exo*nuclease; KF exo) in complex with native or chemically modified DNA reveals steric clashes that likely inhibit enzymatic digestion of the 5′-*C*-methylated ON.[69−72] Given that some of the experiments examining nuclease resistance used oligo-dTs with combined phosphorothioate (PS, ●) and (*S*)-5′-*C* or (*R*)-5′-*C* methylation (Figure 4), we relied on published crystal structures of complexes between KF exo and native 3′-d(GCATTCG)-5′ DNA, or tetramers with either a single *Sp*-PS moiety, 3′-d(T●s_pTTT)-5′, or a single *Rp*-PS moiety, 3′-d(T●$_{Rp}$TTT)-5′.[69] In the structure with the native DNA 7-mer, metal ions A and B are Zn^{2+} and Mg^{2+}, respectively, and in the structure with the *Rp* PS moiety, both ions are Zn^{2+} (Figure 7A). The sulfur atom in the *Sp* configuration results in displacement of both metal ions, and the side chain of Asp-355 is rotated away from the site formerly occupied by metal ion A (Figure 7B).

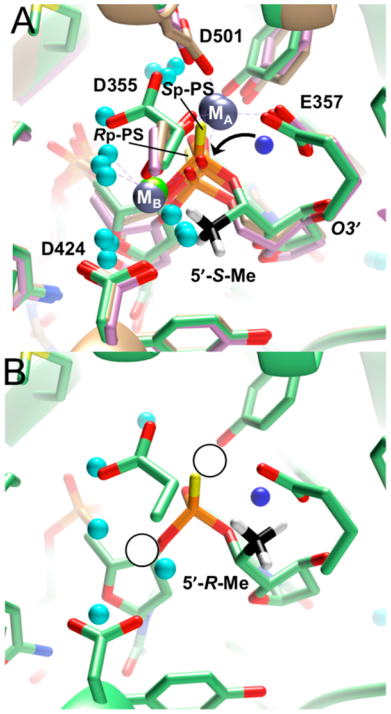

Figure 7. Origins of the increased nuclease resistance of *Sp* PS/(*S*)-5′-*C*-modified ONs compared to the *Rp* PS/(*R*)-5′-*C* isomers. (A) Superimposition of the active sites of Klenow fragment exo domain in complex with 3′-d(GCATTCG)-5′ (beige carbon atoms; metal ion A, M_A = M_B = Zn^{2+}), 3′-d(T●s_pTTT)-5′ with a single *Sp* PS moiety (green carbon atoms; M_A and M_B displaced), or 3′-(T●$_{Rp}$TTT)-5′ a single *Rp* PS moiety (lilac carbon atoms; M_A = Zn^{2+}, M_B = Mg^{2+}).[69] The views are from the 3′-ends of the ONs (O3′ is labeled) onto the last phosphate group. The coordination geometries of metal ions to acidic residues are indicated by dashed lines, and water molecules are cyan spheres, with one of them poised for nucleophilic attack at the phosphate (arrow) in the crystal structure of the complex with native DNA trapped at low pH highlighted in blue. The carbon atom of the modeled (*S*)-5′-*C*-methyl group is highlighted in black with hydrogen atoms added. (B) The active site in the structure of the *Sp* PS-modified DNA from panel A with an additional (*R*)-5′-*C*-methyl modification. The positions of metal ions A and B are indicated with open circles. It is evident that the (*R*)-5′-*C*-methyl group does not interfere with site B. All drawings were generated with the program UCSF Chimera.[73]

As can be seen in Figure 7, when methyl groups are attached at the C5′, the one in (*R*) configuration is directed toward metal ion A and the carboxylate moiety of Glu-357 (Figure 7B). The methyl group in the (*S*)-configuration is directed toward metal ion B (Figure 7A). The combined effects of the PS and 5′-*C*-methyl modifications are interference with metal ion site A (*Sp*-PS/(*R*)-C5′-Me) and both, sites A and B (*Sp*-PS/(*S*)-C5′-Me) (the PS-modified ONs employed in this study represent diastereoisomeric mixtures). Given that both metal ions A (water activation) and B (leaving group stabilization) are important for efficient 3′-5′ exonuclease activity,[67,70] one would predict based on the structural model that the combination of *Sp*-PS with (*S*)-5′-*C*-methylation confers the best protection against nuclease degradation. This is consistent, at least at the qualitative level, with the experimental data shown in Figure 4 and Table 3.

■ CONCLUSIONS

Improved single-step synthesis based on addition of CH_3MgBr to the corresponding 5′-aldehydes and optimized separation and purification protocols of epimers of 2′-substituted 5′-*C*-methyl pyrimidine nucleosides were developed. Detailed structural studies revealed substantial structural similarity of (*S*)-epimers of 5′-*C*-Me nucleosides to their corresponding 5′-unmethylated counterparts with increased C3′-*endo* sugar puckering regardless of 2′-ribo substitution. In contrast, the (*R*)-isomers preferentially exhibited *syn*-nucleobase orientation and prevalent C2′-*endo* sugar puckering. Thermal melting data of 12-mer homo- and heteroduplexes indicated that the spatial orientation of the C5′-methyl is the major determinant of duplex stability. In general, all (*S*)-epimers destabilized duplexes to a lesser degree than the corresponding (*R*)-epimers, consistent with structural similarity of (*S*)-epimers to the corresponding 5′-unmethylated nucleosides.

The (*S*)-isomers with various 2′-substituents provide greater resistance against exonuclease degradation than the corresponding (*R*)-isomers. The X-ray crystal structure analyses of the RNA octamers with (*R*)-C5′-Me-2′-FU and (*S*)-C5′-Me-2′-FU provided insights into the differences in thermal stabilities of duplexes containing these epimers. The model incorporating the spatial structure of the C5′-Me-phosphodiester into the active site of an exonuclease also suggests higher nucleolytic stability for the (*S*)-epimer than the (*R*)-epimer, especially in conjunction with the (*Sp*)-enantiomer of the phosphorothioate.

The X-ray crystal structure and solution-phase NMR data, in addition, consistently support a *gauche*, *gauche* (*sc*+) conformation around the exocyclic C4′−C5′ bond for both 5′-stereoisomers regardless of the nature of the 2′-substitution. This suggests that the Nuclear Overhauser Effect (NOE) between hydrogen atoms of the methyl group and H-3′ in (*R*)-epimers and the absence of the same in the (*S*)-epimers in the NOESY spectra may be used to establish the stereoconfiguration at the C5′ of pyrimidine nucleoside.

Biological evaluation of C5′-methyl nucleosides in the context of siRNAs is in progress. The results from these studies will be published in due course.

■ EXPERIMENTAL SECTION

NMR spectra were recorded on a 400 or 500 MHz instrument for ^1H, a 126 MHz instrument for ^{13}C, a 376 MHz instrument for ^{19}F, and a 162 or 202 MHz instrument for ^{31}P. Chemical shift values for ^1H and ^{13}C are reported in parts per million (δ ppm) using deuterated solvent peak as the reference. α,α,α-Trifluorotoluene and 85% H_3PO_4 were

DOI: 10.1021/acs.joc.5b02375
J. Org. Chem. 2016, 81, 2261−2279

used as external references for ^{19}F and ^{31}P, respectively, and the chemical shift values are reported in ppm. High-resolution mass spectra (HRMS) were recorded in the positive mode by ESI on an iFunnel Q-TOF (time-of-flight) API mass spectrometer. TLC analyses were performed on standard silica-gel 60 F_{254} aluminum plates. Flash chromatography was carried out using standard prepacked silica gel columns. Melting points of the compounds were determined by using a digital melting point apparatus and are uncorrected. X-ray analyses were carried out on a Cu-source diffractometer. Commercially available reagents and anhydrous solvents were used without further purification, unless otherwise noted. 3′-OTBS protected nucleosides **1a**−**d** were prepared in overall yields of 82−95% from the corresponding nucleosides according to published procedures.[74,75] Standard workup implies extraction of product into organic phase, saturated brine wash, drying over anhydrous Na_2SO_4, followed by *in vacuo* evaporation of solvent.

NOESY NMR experiments were run on a 400 MHz instrument with 500 ms mixing time, 0.2 s acquisition time, 1 s delay time (1.2 s total delay time), either 16 or 32 scans per FID, and 400 FIDs all together (raw resolution in the second dimension). Digitization points in the direct observe dimension (first dimension) is 2048. COSY NMR experiments were run on a 400 MHz instrument with 0.2 s acquisition time, 1 s delay time (1.2 s total delay time), 4 scans per FID, and 256 FIDs (raw resolution in the second dimension). Digitization points in the direct observe dimension (first dimension) is 2048.

5′-Deoxy-3′-*O*-[(1,1-dimethylethyl)dimethylsilyl]-2′-*O*-methyl-5′-oxouridine[76] 2a. Dess−Martin periodinane (4.24 g, 10 mmol) was added to a stirred and cooled solution (0 °C) of 3′-OTBS protected uridine **1a** (2.95 g, 7.9 mmol) in anhyd. DCM (120 mL) under Ar atm. The cooling bath was removed, and the mixture was stirred at r.t. for 6 h, after which time no starting alcohol **1a** could be observed by TLC. The mixture was cooled to 0 °C and poured to a vigorously stirred mixture of 5% aq. sodium thiosulfate (75 mL) and saturated aq. $NaHCO_3$ (75 mL). After stirring at r.t. for 20 min, the mixture was extracted with ethyl acetate (EtOAc, 300 mL), and the organic phase was separated, washed with saturated brine, and dried over anhyd. Na_2SO_4. The solvent was removed *in vacuo* at bath temperature not exceeding 25 °C. The residue was dissolved in anhyd. THF, and the solvent was evaporated again to afford 2.79 g (96%) of residue as an amorphous white solid containing ca. 71% of aldehyde **2a** (determined by CHO/NH ratio of H1 NMR in CD_3CN) that was used in the next step without of further purification. The product could be stored at −20 °C under Ar atm. ^1H NMR of major component (400 MHz, CD_3CN): δ 0.15 (s, 6H); 0.93 (s, 9H); 3.37 (s, 3H); 3.62−3.68 (m, 2H); 3.81 (dd, J = 4.6, 5.9 Hz, 1H); 4.48 (d, J = 3.4 Hz, 1H); 4.59 (ddd, J = 0.4, 3.4, 4.5 Hz, 1H); 5.70 (d, J = 8.2 Hz, 1H); 5.94 (d, J = 6.0 Hz, 1H); 7.71 (d, J = 8.2 Hz, 1H); 9.17 (bs, 1H); 9.68 (d, J = 0.5 Hz, 1H).

2′,5′-Dideoxy-3′-*O*-[(1,1-dimethylethyl)dimethylsilyl]-2′-fluoro-5′-oxouridine[77] 2b. 12.7 g (93%) of crude aldehyde **2b** (ca. 60% aldehyde content, an amorphous white solid) was prepared analogously from **1b** (13.8 g, 38 mmol) and DMP (19.5 g, 46 mmol) in anhyd. DCM (550 mL). ^1H NMR of major component (400 MHz, CD_3CN): δ 0.13 (s, 3H); 0.14 (s, 3H); 0.92 (s, 9H); 4.41 (d, J = 6.0 Hz, 1H); 4.67 (ddd, J = 4.9, 6.0, 13.6 [^3JH-F] Hz, 1H, *H3′*); 5.15 (ddd, J = 2.8, 4.9, 52.5 [^2JH-F] Hz, 1H, *H2′*); 5.68 (d, J = 8.1 Hz, 1H); 5.89 (dd, J = 2.8, 18.3 [^3JH-F] Hz, 1H, *H1′*); 7.55 (d, J = 8.1 Hz, 1H); 9.26 (bs, 1H); 9.64 (d, J = 1.0 Hz, 1H).

5′-Deoxy-3′-*O*-[(1,1-dimethylethyl)dimethylsilyl]-5′-oxothymidine[78] 2c. 20.0 g of crude aldehyde **2c** (ca. 63% aldehyde content, an amorphous white solid) was prepared analogously from **1c** (17.9 g, 50 mmol) and DMP (25.4 g, 60 mmol) in anhyd. DCM (500 mL). ^1H NMR of major component (400 MHz, CD_3CN): δ 0.135 (s, 3H); 0.140 (s, 3H); 0.92 (s, 9H); 1.85 (d, J = 1.2 Hz, 3H); 2.08−2.24 (m, 2H); 4.38 (d, J = 2.2 Hz, 1H); 4.75 (dt, J = 2.2, 5.7 Hz, 1H); 6.24 (dd, J = 6.2, 7.9 Hz, 1H); 7.55 (d, J = 1.3 Hz, 1H); 9.18 (bs, 1H); 9.65 (d, J = 0.5 Hz, 1H).

2′,5′-Dideoxy-3′-*O*-[(1,1-dimethylethyl)dimethylsilyl]-5′-oxouridine[79] 2d. 17.0 g (85%) of crude **2d** (ca. 60% aldehyde content, an amorphous white solid) was prepared analogously from **1d** (17.1 g, 50 mmol) and DMP (25 g, 60 mmol) in anhyd. DCM (500 mL). ^1H NMR of major component (400 MHz, CD_3CN): δ 0.08 (s, 3H); 0.09 (s, 3H); 0.86 (s, 9H); 2.04 (ddd, J = 5.6, 7.9, 13.8 Hz, 1H); 2.18 (ddd, J = 2.4, 6.1, 13.8 Hz, 1H); 4.36 (d, J = 2.2 Hz, 1H); 4.70 (dt, J = 2.4, 5.4 Hz, 1H); 5.60 (d, J = 8.1 Hz, 1H); 6.17 (dd, J = 6.0, 7.9 Hz, 1H); 7.70 (d, J = 8.1 Hz, 1H); 9.01 (bs, 1H); 9.59 (d, J = 0.4 Hz, 1H).

5′-(*S*)-*C*-Methyl-3′-*O*-[(1,1-dimethylethyl)dimethylsilyl]-2′-*O*-methyluridine 3a and 5′-(*R*)-*C*-Methyl-3′-*O*-[(1,1-dimethylethyl)dimethylsilyl]-2′-*O*-methyluridine 4a. A solution of crude **2a** with ca.70% aldehyde content (5.45 g, <15 mmol) in anhyd. THF (80 mL) was slowly added via cannula for ca. 20 min to a stirred and cooled (−20 °C) solution of CH_3MgBr (3 M in Et_2O, 20 mL, 60 mmol) in THF (220 mL) under Ar atm. The mixture was stirred at −20 °C for an additional 10 min, the cooling bath was removed, and the reaction was quenched by cautious addition of saturated aq. ammonium chloride (100 mL). The mixture was allowed to warm up to r.t. and diluted with water (20 mL), and the product was extracted into EtOAc (200 mL), followed by standard workup, to obtain 5.73 g of crude product. Flash column chromatography on a 120 g standard prepacked silica gel column using a gradient eluent of 50−80% EtOAc containing 1% of TEA in hexanes afforded prepurified isomers **3a** (2.03 g, 35% based on crude **2a**, ∼79% purity, containing ∼21% of 5′,5′-dimethyl derivative **9a** by ^1H NMR), and **4a** (1.26 g, 22% based on crude **2a**, ∼83% purity, containing ∼17% of primary alcohol **1a** by ^1H NMR) along with a small intermediate mixed fraction. Compound **3a** was used in the next step without further purification. Analytically pure **3a** (18 mg) was prepared by recrystallization of 100 mg of the mixture containing ∼20% **9a** from EtOAc. Compound **4a** contaminated with the nucleoside **1a** was then treated with DMTr-Cl (0.57 g, 1.7 mmol) in anhyd. pyridine (8 mL) under Ar atm for 5 h to convert **1a** to its tritylated derivative. The mixture was quenched by addition of methanol (0.3 mL), and TEA (0.35 mL, 2.3 mmol). Pyridine was evaporated *in vacuo*, and the residue was coevaporated with toluene (30 mL) and partitioned between EtOAc (75 mL) and 5% aq. NaCl (75 mL), followed by standard workup. The residue was dissolved in EtOAc (5 mL), and crystallization was initiated by slow addition of hexanes (20 mL). The mixture was kept overnight at r.t., filtered, washed thoroughly with a 1:10 EtOAc−hexanes mixture and dried to afford pure **4a**, 0.84 g, 15% based on crude **2a**.

Compound **3a**: white crystalline solid, mp (EtOAc), 164−165 °C. ^1H NMR (400 MHz, DMSO-d_6): δ 0.08 (s, 6H); 0.87 (s, 9H); 1.14 (d, J = 6.7 Hz, 3H); 3.33 (s, 3H); 3.68 (dd, J = 1.8, 4.4 Hz, 1H); 3.76−3.84 (m, 2H); 4.27 (t, J = 4.6 Hz, 1H, *H2′*); 5.17 (d, J = 4.4 Hz, 1H, *OH*); 5.65 (d, J = 8.1 Hz, 1H); 5.83 (d, J = 4.7 Hz, 1H, *H1′*); 8.05 (d, J = 8.1 Hz, 1H); 11.3 (s, 1H). ^{13}C NMR (126 MHz, DMSO-d_6): δ −5.0; −4.8; 17.8; 20.1; 25.6; 57.6; 64.7; 70.6; 82.6; 85.8; 88.0; 101.8; 140.2; 150.5; 163.1. HRMS: [M + H]$^+$ calc. for $C_{17}H_{31}N_2O_6Si$, 387.1951; found: 387.1962.

Compound **4a**: white crystalline solid, mp (EtOAc−hexanes), 216−218 °C. ^1H NMR (400 MHz, DMSO-d_6): δ 0.09 (s, 6H); 0.88 (s, 9H); 1.10 (d, J = 6.6 Hz, 3H); 3.28 (s, 3H); 3.64 (dd, J = 2.2, 4.2 Hz, 1H, *H4′*); 3.77 (dt, J = 4.6, 6.5 Hz, 1H, *H5′*); 3.86 (dd, J = 4.8, 6.8 Hz, 1H, *H2′*); 4.40 (dd, J = 2.2, 4.7 Hz, 1H, *H3′*); 5.16 (d, J = 4.9 Hz, 1H, *OH*); 5.67 (dd, J = 2.2, 8.1 Hz, 1H); 5.86 (d, J = 6.8 Hz, 1H, *H1′*); 7.89 (d, J = 8.2 Hz, 1H); 11.36 (d, J = 1.8 Hz, 1H). ^{13}C NMR (126 MHz, DMSO-d_6): δ 0.6; 0.7; 23.2; 25.2; 62.8; 71.5; 74.5; 87.1; 90.5; 94.8; 107.7; 145.9; 156.1; 168.4. HRMS: [M + H]$^+$ calc. for $C_{17}H_{31}N_2O_6Si$, 387.1951; found: 387.1960.

5′-(*S*)-*C*-Methyl-2′-deoxy-3′-*O*-[(1,1-dimethylethyl)dimethylsilyl]-2′-fluorouridine 3b and 5′-(*R*)-*C*-Methyl-2′-deoxy-3′-*O*-[(1,1-dimethylethyl)dimethylsilyl]-2′-fluorouridine 4b. Compounds **3b** (3.43 g, 78% containing ∼22% of 5′,5′-dimethyl derivative **9b**) and **4b** (2.55 g, 14%) were analogously prepared by addition of a solution of crude **2b** with ca. 60% aldehyde content (18.3 g, <51 mmol) in anhyd. THF (250 mL) to CH_3MgBr (3 M in Et_2O, 67 mL, 200 mmol) in anhyd. THF (700 mL) at −20 °C for 10 min, followed by stirring at −20 °C for 30 min. The crude residue (18.1 g) in EtOAc (100 mL) was stirred overnight, and the precipitate was filtered and washed with a small amount of EtOAc to afford 0.94 g of prepurified

DOI: 10.1021/acs.joc.5b02375
J. Org. Chem. 2016, 81, 2261−2279

(*R*)-isomer **4b**. The mother liquor was evaporated, and the residue was chromatographed over a standard prepacked silica gel column (330 g) using a gradient eluent of 50−90% EtOAc containing 1% of TEA in hexanes to afford prepurified **3b** (3.43 g, ∼78% purity, containing ∼22% of 5′,5′-dimethyl derivative **9b**), and **4b** (3.20 g). Combined prepurified **4b** (4.10 g) was recrystallized from 80 mL of hot EtOAc to afford 2.04 g of pure **4b**. Prepurified **3b** could be used in the next step without further purification. Analytically pure **3b** (27 mg) was prepared by recrystallization of 100 mg of the prepurified mixture from 4 mL of a hot 1:1 EtOAc−hexanes mixture.

Compound **3b**: white crystalline solid, mp (EtOAc−hexanes), 167−168 °C. ^{1}H NMR (400 MHz, DMSO-d_6): δ 0.088 (s, 3H); 0.094 (s, 3H); 0.86 (s, 9H); 1.19 (d, J = 6.5 Hz, 3H); 3.72 (d, J = 6.8 Hz, 1H); 3.75−3.83 (m, 1H); 4.31 (ddd, J = 4.4, 6.8, 18.3 [^{3}JH-F] Hz, 1H, *H3′*); 5.06 (ddd, J = 2.4, 4.4, 53.1 [^{2}JH-F] Hz, 1H, *H2′*); 5.20 (d, J = 4.7 Hz, 1H, *OH*); 5.63 (d, J = 8.1 Hz, 1H); 5.91 (dd, J = 2.3, 16.9 [^{3}JH-F] Hz, 1H, *H1′*); 7.99 (d, J = 8.1 Hz, 1H); 11.4 (s, 1H). ^{13}C NMR (126 MHz, acetone-d_6): δ −4.8; −4.5; 18.8; 20.7; 26.1; 66.0; 71.3; 71.4; 88.0; 88.5; 88.8; 93.9 (d, ^{1}JC-F = 191 Hz); 102.6; 141.4; 151.4; 163.7. ^{19}F NMR (376 MHz, acetone-d_6): δ −207.60 (dt, J = 16.6, 53.1 Hz, 1F). HRMS: [M + H]$^+$ calc. for $C_{16}H_{28}FN_2O_5Si$, 375.1752; found: 375.1744.

Compound **4b**: white crystalline solid, mp (EtOAc), 224−226 °C. ^{1}H NMR (400 MHz, DMSO-d_6): δ 0.096 (s, 3H); 0.102 (s, 3H); 0.87 (s, 9H); 1.11 (d, J = 6.7 Hz, 3H); 3.74−3.78 (m, 1H); 3.84−3.94 (m, 1H); 4.43 (dt, J = 4.8, 12.2 [^{3}JH-F] Hz, 1H, *H3′*); 5.10 (dt, J = 4.2, 52.8 [^{2}JH-F] Hz, 1H, *H2′*); 5.21 (d, J = 4.7 Hz, 1H, *OH*); 5.65 (d, J = 8.1 Hz, 1H); 5.94 (dd, J = 4.0, 15.8 [^{3}JH-F] Hz, 1H, *H1′*); 7.89 (d, J = 8.1 Hz, 1H); 11.4 (s, 1H). ^{13}C NMR (126 MHz, CD_3OD): δ −4.6; −4.1; 19.1; 19.9; 26.5; 67. 7; 70.6; 70.7; 88.3; 88.6; 90.0; 93.7 (d, ^{1}JC-F = 192 Hz); 103.4; 142.7; 152.3; 165.7. ^{19}F NMR (376 MHz, acetone-d_6): δ −208.28 (dt, J = 14.3, 52.8 Hz, 1F). HRMS: [M + H]$^+$ calc. for $C_{16}H_{28}FN_2O_5Si$, 375.1752; found: 375.1760.

5′-(*S*)-*C*-Methyl-3′-*O*-[(1,1-dimethylethyl)dimethylsilyl]-thymidine[80] 3c and 5′-(*R*)-*C*-Methyl-3′-*O*-[(1,1-dimethylethyl)-dimethylsilyl]-thymidine[80] 4c. Prepurified (*S*)-isomer **3c** (4.34 g, ∼95% purity, containing ∼5% of 5′,5′-dimethyl derivative **9c**, 26% based on crude **2c**) and pure (*R*)-isomer **4c**: 2.34 g (14% based on crude **2c**) were analogously prepared by addition of a solution of crude aldehyde **2c** containing ca. 60% of the title compound (18.0 g, <50 mmol) in anhyd. THF (250 mL) to a solution of CH_3MgBr (3 M in Et_2O, 67 mL, 200 mmol) in anhyd. THF (700 mL) at −20 °C for 10 min, followed by stirring at −20 °C for 60 min. The crude residue (17.7 g) was successively chromatographed 4 times over standard prepacked silica gel flash-columns (330, 220, 80, and 40 g) using a gradient eluent of 80−100% ethyl ether containing 1% of TEA in hexanes. The fractions containing separated epimers were pulled out, and intermediate mixed fractions were combined and subjected to repeated column chromatography to achieve complete separation of the epimers. Analytically pure **3c** with no detectable 5′,5′-dimethyl derivative contaminant **9c** was separated from column fractions for characterization.

Compound **3c**: an amorphous white solid. ^{1}H NMR (400 MHz, DMSO-d_6): δ 0.07 (s, 6H); 0.86 (s, 9H); 1.13 (d, J = 6.5 Hz, 3H); 1.76 (d, J = 1.0 Hz, 3H); 2.01 (ddd, J = 3.0, 6.0, 13.2 Hz, 1H, $H2'_A$); 2.13 (ddd, J = 5.9, 7.7, 13.4 Hz, 1H, $H2'_B$); 3.58 (t, J = 2.7 Hz, 1H, *H4′*); 3.74−3.83 (m, 1H, *H5′*); 4.40 (quintet, J = 2.8 Hz, 1H, *H3′*); 5.02 (d, J = 4.6 Hz, 1H, *OH*); 6.15 (dd, J = 6.0, 7.7 Hz, 1H, *H1′*); 7.84 (d, J = 1.2 Hz, 1H); 11.27 (s, 1H). ^{13}C NMR (126 MHz, CD_3CN): δ −4.6; −4.4; 12.7; 18.6; 20.7; 26.2; 41.1; 67.6; 73.9; 86.0; 97.7; 111.1; 137.9; 151.8; 165.1. HRMS: [M + Na]$^+$ calc. for $C_{17}H_{30}N_2NaO_5$, 393.1822; found: 393.1825.

Compound **4c**: an amorphous white solid. ^{1}H NMR (400 MHz, DMSO-d_6): δ 0.081 (s, 3H); 0.084 (s, 3H); 0.87 (s, 9H); 1.10 (d, J = 6.5 Hz, 3H); 1.76 (d, J = 1.1 Hz, 3H); 1.95 (ddd, J = 1.7, 5.5, 13.1 Hz, 1H, $H2'_A$); 2.14 (ddd, J = 5.4, 9.0, 13.2 Hz, 1H, $H2'_B$); 3.55 (dd, J = 1.6, 4.7 Hz, 1H, *H4′*); 3.73 (dt, J = 4.9, 6.4 Hz, 1H, *H5′*); 4.49 (dt, J = 1.4, 5.3 Hz, 1H, *H3′*); 5.03 (d, J = 5.0 Hz, 1H, *OH*); 6.15 (dd, J = 5.5, 8.9 Hz, 1H, *H1′*); 7.66 (d, J = 1.2 Hz, 1H); 11.29 (s, 1H). ^{13}C NMR (126 MHz, CD_3CN): δ −4.5; −4.3; 12.7; 18.6; 20.2; 26.2; 41.1; 68.3; 72.5; 86.1; 92.4; 111.3; 137.8; 151.8; 165.1. HRMS: [M + H]$^+$ calc. for $C_{17}H_{31}N_2O_5Si$, 371.2002; found: 371.1992.

5′-(*S*)-*C*-Methyl-2′-deoxy-3′-*O*-[(1,1-dimethylethyl)dimethylsilyl]-uridine 3d and 5′-(*R*)-*C*-Methyl-2′-deoxy-3′-*O*-[(1,1-dimethylethyl)dimethylsilyl]-uridine 4d. Prepurified (*S*)-isomer **3d** (4.60 g, ∼91% purity, containing ∼9% of 5′,5′-dimethyl derivative **9d**, yield: 27% based on crude **2d**) and pure (*R*)-isomer **4d** as (2.20 g, 13% based on crude **2d**) were analogously prepared by addition of a solution of crude aldehyde **2d** containing ca. 60% of the title compound (17.0 g, <50 mmol) in anhyd. THF (200 mL) to a solution of CH_3MgBr (3 M in Et_2O, 67 mL, 200 mmol) in anhyd. THF (700 mL) at −20 °C for 10 min, followed by stirring at −20 °C for 2 h. The crude residue (15.6 g) was successively chromatographed thrice over standard prepacked silica gel flash-columns (330, 220, and 80 g) with a gradient of 80−100% ethyl ether containing 1% of TEA in hexanes. The fractions containing fully separated epimers were pulled, and intermediate mixed fractions were combined and subjected to repeated column chromatography to achieve complete separation of the epimers. The prepurified 95% pure **3d** could be used for the next step without further purification. The analytically pure sample of **3d** was obtained by crystallization from acetonitrile.

Compound **3d**: white crystalline solid, mp (MeCN) 164−166 °C. ^{1}H NMR (400 MHz, DMSO-d_6): δ 0.07 (s, 6H); 0.86 (s, 9H); 1.12 (d, J = 6.4 Hz, 3H); 2.05 (ddd, J = 3.2, 6.1, 13.2 Hz, 1H, $H2'_A$); 2.12 (ddd, J = 5.7, 7.2, 13.1 Hz, 1H, $H2'_B$); 3.60 (t, J = 2.6 Hz, 1H); 3.74−3.82 (m, 1H); 4.40 (quintet, J = 2.8, 1H, *H3′*); 5.04 (d, J = 4.6 Hz, 1H, *OH*); 5.65 (d, J = 8.1 Hz, 1H); 6.15 (t, J = 6.4 Hz, 1H, *H1′*); 7.99 (d, J = 8.1 Hz, 1H); 11.28 (s, 1H). ^{13}C NMR (126 MHz, DMSO-d_6): δ −4.9; −4.8; 17.6; 20.1; 25.6; 40.2; 65.5; 72.9; 83.8; 90.5; 101.8; 140.4; 150.4; 163.1. HRMS: [M + H]$^+$ calc. for $C_{16}H_{29}N_2O_5Si$, 357.1846; found: 357.1841

Compound **4d**: white crystalline solid, mp (ether−hexanes) 208−210 °C. ^{1}H NMR (400 MHz, DMSO-d_6): δ 0.080 (s, 3H); 0.084 (s, 3H); 0.87 (s, 9H); 1.10 (d, J = 6.4 Hz, 3H); 2.00 (ddd, J = 1.7, 5.6, 13.1 Hz, 1H, $H2'_A$); 2.11 (ddd, J = 5.4, 8.7, 13.4 Hz, 1H, $H2'_B$); 3.56 (dd, J = 1.5, 4.8 Hz, 1H, *H5′*); 3.71 (td, J = 6.0, 11.2 Hz, 1H, *H4′*); 4.49 (dd, J = 2.0, 5.2 Hz, 1H, *H3′*); 5.00 (d, J = 5.1 Hz, 1H, *OH*); 5.64 (d, J = 8.1 Hz, 1H); 6.14 (dd, J = 5.7, 8.6 Hz, 1H, *H1′*); 7.80 (d, J = 8.1 Hz, 1H); 11.30 (s, 1H). ^{13}C NMR (126 MHz, DMSO-d_6): δ −4.9; −4.7; 17.6; 19.9; 25.6; 66.3; 71.6; 83.9; 91.2; 102.0; 140.5; 150.5; 163.0. HRMS: [M + H]$^+$ calc. for $C_{16}H_{29}N_2O_5Si$, 357.1846; found: 357.1837.

5′-(*S*)-*C*-Methyl-5′-*O*-[bis(4-methoxyphenyl)phenylmethyl]-2′-*O*-methyluridine 5a. A mixture of prepurified (*S*)-isomer **3a** (∼79% purity, containing ∼21% of 5′,5′-dimethyl derivative **9a**, 2.24 g, ∼5.8 mmol of **3a**), DMTr-Cl (3.73 g, 11 mmol), $AgNO_3$ (1.70 g, 10 mmol), and pyridine (22 mL) in anhyd. THF (90 mL) was stirred at r.t. under Ar atm for 42 h, quenched by addition of 0.3 mL of MeOH, and diluted with toluene (100 mL). After stirring for an additional 1 h, the mixture was filtered through Celite, and the Celite plug was washed thoroughly with toluene. The filtrate was evaporated *in vacuo* to afford 8.20 g of residue that was dissolved in anhyd. THF (40 mL) under Ar atm, and tetrabutylammonium fluoride (TBAF, 1 M in THF, 11 mL, 11 mmol) was added. The mixture was stirred at r.t. under Ar atm for 23 h and evaporated *in vacuo*, and the residue was partitioned between EtOAc (200 mL) and 5% aq. NaCl (200 mL), followed by standard workup, to obtain 5.76 g of crude residue. Flash chromatography of the residue over a column of silica gel with a gradient eluent of 70−100% EtOAc in hexanes yielded 3.13 g of pure **5a** as an amorphous white foam (94% based on **3a** content). ^{1}H NMR (400 MHz, DMSO-d_6): δ 0.68 (d, J = 6.3 Hz, 3H); 3.35 (s, 3H); 3.51−3.58 (m, 1H); 3.726 (s, 3H), 3.731 (s, 3H); 3.74 (t, J = 4.6 Hz, 1H); 3.78 (t, J = 5.6 Hz, 1H); 4.14 (q, J = 6.3 Hz, 1H); 5.09 (d, J = 6.7 Hz, 1H); 5.57 (d, J = 8.1 Hz, 1H); 5.77 (d, J = 5.7 Hz, 1H); 6.84−6.91 (m, 4H); 7.18−7.23 (m, 1H); 7.26−7.34 (m, 6H); 7.40−7.45 (m, 2H); 7.61 (d, J = 8.1 Hz, 1H); 11.41 (s, 1H). ^{13}C NMR (126 MHz, CD_3CN): δ 18.4; 50.0; 59.1; 69.7; 70.7; 84.0; 87.6; 87.76; 87.79; 88.3; 102.9; 102.9; 114.0; 127. 9; 128.7; 129.4; 131.5, 131.3; 137.7; 137.9; 141.2; 147.5; 151.5; 159.8; 159.8; 164.3. HRMS: [M + Na]$^+$ calc. for $C_{32}H_{34}N_2NaO_8$, 597.2213; found: 597.2211.

DOI: 10.1021/acs.joc.5b02375
J. Org. Chem. 2016, 81, 2261−2279

Isolation of Side Product 5′,5′-*C*-Dimethyl-3′-*O*-[(1,1-dimethylethyl)dimethylsilyl]-2′-*O*-methyluridine 9a. Because of the presence of inseparable unreacted residual starting material **3a** from the tritylation reaction, the desired purity for **9a** could not be achieved. A 3:2 mixture of **9a** and **3a** (0.27 g) was isolated from the reaction of prepurified (*S*)-isomer **3a** (~85% purity, containing ~15% of 5′,5′-dimethyl derivative **9a**, 1.07 g, 2.8 mmol), DMTr-Cl (1.42 g, 4.2 mmol), $AgNO_3$ (0.65 g, 3.8 mmol), and pyridine (8.4 mL) in anhyd. THF (35 mL) as described above. Silica gel column chromatography using a gradient eluent of 70−100% EtOAc in hexanes afforded compound **5a** as an amorphous white foam (1.31g, 85%) and 0.27 g of a 3:2 mixture of **9a** and **3a**. The 3:2 mixture of **9a** and **3a** was analyzed by ^{1}H NMR and HRMS to establish the identity of compound **9a**. ^{1}H NMR of major component (**9a**) (400 MHz, DMSO-d_6): δ 0.089 (s, 3H); 0.093 (s, 3H); 0.87 (s, 9H); 1.13 (s, 3H); 1.18 (s, 3H); 3.27 (s, 3H); 3.60 (d, J = 2.1 Hz, 1H); 3.77−3.83 (m, 1H); 4.39 (dd, J = 2.2, 4.7 Hz, 1H); 4.93 (s, 1H); 5.69 (d, J = 8.1 Hz, 1H); 5.88 (d, J = 6.6 Hz, 1H); 8.05 (d, J = 8.1 Hz, 1H); 11.36 (bs, 1H). HRMS: $[M + H]^+$ calc. for $C_{18}H_{33}N_2O_6Si$, 401.2108; found: 401.2112.

5′-(*S*)-*C*-Methyl-5′-*O*-[bis(4-methoxyphenyl)phenylmethyl]-2′-deoxy-2′-fluorouridine 5b. 0.78 g of pure **5b** (97% based on **3b** content) was prepared analogously from prepurified (*S*)-isomer **3b** (~81% purity, containing ~19% of 5′,5′-dimethyl derivative **9b**, 4.06 g, ~8.8 mmol of **3b**), DMTr-Cl (5.76 g, 17 mmol), $AgNO_3$ (2.55 g, 15 mmol), and pyridine (35 mL) in anhyd. THF (140 mL). After filtration and evaporation, the crude residue was treated with TBAF (1 M in THF, 17 mL, 17 mmol) in anhyd. THF (60 mL), followed by standard workup and flash column chromatography on silica gel with a gradient eluent of 70−100% EtOAc and hexanes, to afford desired compound **5b** as an amorphous white foam. ^{1}H NMR (400 MHz, DMSO-d_6): δ 0.66 (d, J = 6.3 Hz, 3H); 3.49−3.58 (m, 1H); 3.68 (s, 3H); 3.69 (s, 3H); 3.74 (dd, J = 4.7, 7.7 Hz, 1H); 4.15−4.27 (m, 1H); 5.07 (ddd, J = 2.1, 5.0, 53.1 [^2JH-F] Hz, 1H, *H2′*); 5.40 (d, J = 7.1 Hz, 1H); 5.49 (d, J = 8.1 Hz, 1H); 5.78 (dd, J = 2.1, 19.4 [^3JH-F] Hz, 1H, *H1′*); 6.82 (t split, J = 8.4 Hz, 4H); 7.13−7.19 (m, 1H); 7.20−7.31 (m, 6H); 7.39 (d split, J = 7.2 Hz, 2H); 7.61 (d, J = 8.0 Hz, 1H); 11.40 (s, 1H). ^{13}C NMR (126 MHz, acetone-d_6): δ 54.6; 68.8; 69.0; 69.4; 85.8, 86.5; 88.4; 88.8; 93.6 (d, ^1JC-F = 186 Hz); 101.8; 112.8; 126.6; 127.5; 128.4; 130.6; 130.6; 136.6; 136.8; 140.6; 146.6; 150.2; 158.7; 158.8; 162.8. ^{19}F NMR (376 MHz, acetone-d_6): δ −204.30 (dt, J = 19.0, 53.2 Hz, 1F). HRMS: $[M + Na]^+$ calc. for $C_{31}H_{31}FN_2NaO_7$, 585.2013; found: 585.2001.

5′-(*S*)-*C*-Methyl-5′-*O*-[bis(4-methoxyphenyl)phenylmethyl]-thymidine 5c. 0.99 g (96%) of pure **5c** was prepared analogously from prepurified (*S*)-isomer **3c** (~96% purity, containing ~4% of 5′,5′-dimethyl derivative **9c**, 4.27 g, ~11 mmol of **3c**), DMTr-Cl (5.76 g, 17 mmol), $AgNO_3$ (2.55 g, 15 mmol), and pyridine (34 mL) in anhyd. THF (140 mL). After filtration and evaporation, crude residue was treated with TBAF (1 M in THF, 17 mL, 17 mmol) in anhyd. THF (50 mL), followed by standard workup and flash column chromatography on silica gel with a gradient eluent of 70−100% EtOAc in hexanes, to afford compound **5c** as an amorphous white foam. ^{1}H NMR (400 MHz, CD_3CN): δ 0.86 (d, J = 6.3 Hz, 3H); 1.75 (d, J = 1.2 Hz, 3H); 2.18 (dd, J = 5.2, 6.8 Hz, 2H); 3.29 (bs, 1H); 3.56−3.63 (m, 1H); 3.64 (t, J = 3.8 Hz, 1H); 3.749 (s, 3H); 3.756 (s, 3H); 4.33 (dd, J = 5.2, 8.9 Hz, 1H); 6.14 (t, J = 6.9 Hz, 1H); 6.82−6.89 (m, 4H); 7.18−7.23 (m, 1H); 7.25−7.31 (m, 2H); 7.36−7.43 (m, 4H); 7.49−7.53 (m, 2H); 7.56 (d, J = 1.2 Hz, 1H); 9.60 (bs, 1H). ^{13}C NMR (126 MHz, CD_3CN): δ 12.7; 18.4; 41.4; 56.0; 71.0; 71.6; 85.1; 87.6; 90.6; 111.3; 114.0; 127.9; 128.7; 129.3; 131.4; 131.6; 136.8; 137.7; 138.0; 147.5; 151.6; 159.8; 159.8; 165.1. HRMS: $[M + Na]^+$ calc. for $C_{32}H_{34}N_2NaO_7$, 581.2264; found: 581.2269.

5′-(*S*)-*C*-Methyl-5′-*O*-[bis(4-methoxyphenyl)phenylmethyl]-2′-deoxyuridine 5d. 2.56 g (96%) of **5d** was prepared analogously from prepurified (*S*)-isomer **3d** (~91% purity, containing ~9% of 5′,5′-dimethyl derivative **9d**, 1.86 g, 4.7 mmol of **3d**), DMTr-Cl (2.60 g, 7.7 mmol), $AgNO_3$ (1.19 g, 7.0 mmol), and pyridine (15 mL) in anhyd. THF (60 mL). After filtration and evaporation, the crude residue was treated with TBAF (1 M in THF, 8 mL, 8 mmol) in anhyd. THF (20 mL), followed by standard workup and flash column chromatography on silica gel with a gradient eluent of 70−100% EtOAc in hexanes, to afford compound **5d** as an amorphous white foam. ^{1}H NMR (500 MHz, DMSO-d_6): δ 0.66 (d, J = 6.3 Hz, 3H); 2.04−2.14 (m, 2H); 3.55 (quintet, J = 6.0 Hz, 1H); 3.65−3.70 (m, 1H); 3.729 (s, 3H); 3.733 (s, 3H); 4.20−4.26 (m, 1H); 5.21 (bs, 1H); 5.58 (d, J = 8.1 Hz, 1H); 6.06 (t, J = 6.9 Hz, 1H); 6.86 (d, J = 7.5 Hz, 2H); 6.88 (d, J = 7.6 Hz, 2H); 7.18−7.22 (m, 1H); 7.25−7.33 (m, 6H); 7.42 (d, J = 7.6 Hz, 2H); 7.59 (d, J = 8.1 Hz, 1H); 11.32 (s, 1H). ^{13}C NMR (126 MHz, DMSO-d_6): δ 17.1; 54.9; 69.5; 69.7; 83.6; 85.8; 88.8; 101.7; 112.9; 126.5; 127.5; 127.9; 130.0; 130.1; 136.3; 136.4; 140.0; 146.1; 150.3; 158.0; 158.1; 162.9. HRMS: $[M + Na]^+$ calc. for $C_{31}H_{32}N_2NaO_7$, 567.2107; found: 567.2111.

5′-(*R*)-*C*-Methyl-5′-*O*-[bis(4-methoxyphenyl)phenylmethyl]-2′-*O*-methyluridine 6a. 1.66 g (96%) of pure **6a** was prepared analogously from (*R*)-isomer **4a** (1.15 g, 3 mmol), DMTr-Cl (1.53 g, 4.5 mmol), $AgNO_3$ (0.70 g, 4.1 mmol), and pyridine (9 mL) in anhyd. THF (40 mL). After filtration and evaporation, the crude residue was treated with TBAF (1 M in THF, 4.5 mL, 4.5 mmol) in anhyd. THF (20 mL), followed by standard workup and flash column chromatography on silica gel with a gradient eluent of 70−100% EtOAc in hexanes, to afford compound **6a** as an amorphous white foam. ^{1}H NMR (400 MHz, DMSO-d_6): δ 0.80 (d, J = 6.4 Hz, 3H); 3.34 (s, 3H); 3.43−3.51 (m, 1H); 3.68 (t, J = 5.7 Hz, 1H); 3.70 (dd, J = 3.2, 4.5 Hz, 1H); 3.74 (s, 6H); 4.31 (dd, J = 5.7, 10.9 Hz, 1H); 5.16−5.20 (m, 2H); 5.75 (d, J = 5.7 Hz, 1H); 6.90 (d split, J = 9.0 Hz, 4H); 7.19−7.25 (m, 1H); 7.28−7.36 (m, 7H); 7.42−7.47 (m, 2H); 11.39 (d, J = 1.9 Hz, 1H). ^{13}C NMR (126 MHz, CD_3CN): δ 18.2; 56.0; 59.1; 69.4; 70.8; 83.6; 87.4; 87.8; 88.4; 102.9; 114.1; 114.1; 127.9; 128.8; 129.3; 131.5; 131.6; 137.4; 137.7; 141.5; 147.6; 151.5; 159.8; 164.1. HRMS: $[M + Na]^+$ calc. for $C_{32}H_{34}N_2NaO_8$, 597.2213; found: 597.2208.

5′-(*R*)-*C*-Methyl-5′-*O*-[bis(4-methoxyphenyl)phenylmethyl]-2′-deoxy-2′-fluorouridine 6b. 3.80 g (99%) of pure **6b** was prepared analogously from (*R*)-isomer **4b** (2.55 g, 6.9 mmol), DMTr-Cl (3.39 g, 10 mmol), $AgNO_3$ (1.53 g, 9 mmol), and pyridine (20 mL) in anhyd. THF (90 mL). After filtration and evaporation, the crude residue was treated with TBAF (1 M in THF, 11 mL, 11 mmol) in anhyd. THF (40 mL), followed by standard workup and flash column chromatography on silica gel with a gradient eluent of 70−100% EtOAc in hexanes, to afford compound **6b** as an amorphous white foam. ^{1}H NMR (400 MHz, DMSO-d_6): δ 0.69 (d, J = 6.5 Hz, 3H); 3.58−3.65 (m, 1H); 3.66−3.72 (m, 1H); 3.69 (s, 6H); 4.31−4.44 (m, 1H); 5.06 (ddd, J = 2.0, 5.1, 53.7 [^2JH-F] Hz, 1H, *H2′*); 5.21 (d, J = 8.0 Hz, 1H); 5.53 (d, J = 6.9 Hz, 1H); 5.73 (dd, J = 2.0, 21.5 [^3JH-F] Hz, 1H, *H1′*); 6.81−6.87 (m, 4H); 7.14−7.19 (m, 1H); 7.21−7.31 (m, 6H); 7.37−7.42 (m, 2H); 7.52 (d, J = 8.1 Hz, 1H); 11.38 (s, 1H). ^{13}C NMR (126 MHz, acetone-d_6): δ 17.6; 55.6; 69.8; 70.0; 70.2; 86.4; 87.7; 89.0; 89.3; 94.2 (d, ^1JC-F = 187 Hz); 102.8; 113.9; 114.0; 127.6; 128.6; 129.3; 131.5; 131.5; 137.5; 137.6; 142.0; 147.6; 151.2; 159.8; 163.5. ^{19}F NMR (376 MHz, acetone-d_6): δ −204.92 (dt, J = 18.5, 53.4 Hz, 1F). HRMS: $[M + Na]^+$ calc. for $C_{31}H_{31}FN_2NaO_7$, 585.2013; found: 585.2030.

5′-(*R*)-*C*-Methyl-5′-*O*-[bis(4-methoxyphenyl)phenylmethyl]-thymidine 6c. 2.82 g (99%) of pure **6c** was prepared analogously from (*R*)-isomer **4c** (1.90 g, 5.1 mmol), DMTr-Cl (2.61 g, 7.7 mmol), $AgNO_3$ (1.19 g, 7 mmol), and pyridine (15 mL) in anhyd. THF (60 mL). After filtration and evaporation, the crude residue was treated with TBAF (1 M in THF, 8 mL, 8 mmol) in anhyd. THF (20 mL), followed by standard workup and flash column chromatography on silica gel with a gradient of 70−100% EtOAc in hexanes, to afford compound **6c** as an amorphous white foam. ^{1}H NMR (500 MHz, CD_3CN): δ 0.88 (d, J = 6.4 Hz, 3H); 1.45 (d, J = 1.3 Hz, 3H); 2.06 (ddd, J = 6.5, 8.5, 13.8 Hz, 1H); 2.12 (ddd, J = 2.5, 6.0, 13.6 Hz, 1H); 3.37−3.43 (m, 2H); 3.65 (t, J = 3.4 Hz, 1H); 3.745 (s, 3H); 3.753 (s, 3H); 4.59−4.64 (m, 1H); 6.17 (dd, J = 5.9, 8.5 Hz, 1H); 6.83−6.89 (m, 4H); 7.03 (d, J = 1.3 Hz, 1H); 7.20 (tt, J = 1.3, 7.3 Hz, 1H); 7.26−7.31 (m, 2H); 7.38−7.44 (m, 4H); 7.52−7.55 (m, 2H); 9.43 (s, 1H). ^{13}C NMR (126 MHz, CD_3CN): δ 12.3; 18.4; 40.5; 56.0; 71.3; 71.5; 84.5; 87.4; 90.9; 111.4; 114.0; 114.1; 127.9; 128.8; 129.2; 131.3; 131.5;

DOI: 10.1021/acs.joc.5b02375
J. Org. Chem. 2016, 81, 2261−2279

136.6; 137.8; 138.2; 147.8; 151.6; 159.79; 159.8; 164.8. HRMS: [M + Na]$^+$ calc. for $C_{32}H_{34}N_2NaO_7$, 581.2264; found: 581.2269.

5′-(*R*)-*C*-Methyl-5′-*O*-[bis(4-methoxyphenyl)phenylmethyl]-2′-deoxyuridine 6d. 1.60 g (57%) of pure **6d** was prepared analogously from (*R*)-isomer **4d** (1.86 g, 5.2 mmol), DMTr-Cl (2.6 g, 7.7 mmol), $AgNO_3$ (1.19 g, 7 mmol), and pyridine (15 mL) in anhyd. THF (60 mL). After filtration and evaporation, the crude residue was treated with TBAF (1 M in THF, 8 mL, 8 mmol) in anhyd. THF (20 mL), followed by standard workup and flash column chromatography on silica gel with a gradient of 70−100% EtOAc in hexanes, to afford compound **6d** as an amorphous white foam. ^{1}H NMR (400 MHz, $CDCl_3$): δ 1.03 (d, J = 6.4 Hz, 3H); 1.98−2.07 (m, 1H); 2.27−2.35 (m, 1H); 2.71 (d, J = 5.1 Hz, 1H); 3.37−3.44 (m, 1H); 3.69 (dd, J = 5.0, 5.5 Hz, 1H); 3.779 (s, 3H); 3.782 (s, 3H); 4.51 (quintet, J = 4.5 Hz, 1H); 5.28 (dd, J = 2.7, 10.2 Hz, 1H); 6.24 (dd, J = 7.8, 9.0 Hz, 1H); 6.80−6.86 (m, 4H); 7.08 (d, J = 10.2 Hz, 1H); 7.14−7.22 (m, 1H); 7.24−7.31 (m, 6H); 7.47 (d, J = 7.1 Hz, 2H); 9.08 (s, 1H). ^{13}C NMR (126 MHz, $CDCl_3$): δ 19.0; 40.8; 55.4; 71.0; 71.5; 77.0; 77.2; 77.5; 81.6; 84.1; 87.2; 113.3; 127.1; 127.2; 127.96; 128.0; 128.1; 128.2; 129.3; 130.5; 130.6; 136.4; 136.5; 139.7; 146.4; 147.6; 158.8; 158.9. HRMS: [M + Na]$^+$ calc. for $C_{31}H_{32}N_2NaO_7$, 567.2107; found: 567.2117.

5′-(*S*)-*C*-Methylthymidine[49] 7c. Compound **5c** (240 mg, 0.44 mmol) was dissolved in anhyd. EtOH (3 mL), and one drop of conc. aq. HCl was added. The solution was kept at r.t. for 30 min, and diluted with toluene (6 mL), and the solvents were removed *in vacuo*. The residue was coevaporated with a 1:2 mixture of EtOH−toluene, and triturated with 4 mL of diethyl ether. After staying overnight at r.t., the crystalline residue was filtered, thoroughly washed with diethyl ether, and dried to afford 102 mg (90%) of **7c** as a white crystalline solid; mp (ether) 214−216 °C (decomp), mp reported 201−202 °C.[49] ^{1}H NMR (400 MHz, DMSO-d_6): δ 1.12 (d, J = 6.5 Hz, 3H); 1.75 (d, J = 1.1 Hz, 3H); 1.99−2.09 (m, 1H); 3.56 (t, J = 2.9 Hz, 1H); 3.78 (dd, J = 3.0, 6.4 Hz, 1H); 4.19−4.25 (m, 1H); 4.95 (bs, 1H, *OH*); 5.16 (bs, 1H, *OH*); 6.17 (t, J = 6.6 Hz, 1H, *H1′*); 7.87 (d, J = 1.2 Hz, 1H); 11.25 (s, 1H). ^{13}C NMR (126 MHz, DMSO-d_6): δ 12.4; 20.2; 56.0; 66.0; 71.2; 83.7; 90.3; 109.2; 136.3; 150.5; 163.8. HRMS: [M + H]$^+$ calc. for $C_{11}H_{17}N_2O_5$, 257.1137; found: 257.1142.

5′-(*S*)-*C*-Methyl-2′-*O*-methyluridine 7a. 13 mg (59%) of pure **7a** as an amorphous white solid was prepared analogously from compound **5a** (45 mg, 0.08 mmol). ^{1}H NMR (400 MHz, DMSO-d_6): δ 1.12 (d, J = 6.4 Hz, 3H); 3.33 (s, 3H); 3.65−3.70 (m, 1H); 3.76 (t, J = 5.1 Hz, 1H); 3.76−3.84 (m, 1H); 4.09 (bs, 1H); 5.08 (bs, 1H, *OH*); 5.12 (bs, 1H, *OH*); 5.65 (dd, J = 1.7, 7.8 Hz, 1H); 5.86 (d, J = 5.0 Hz, 1H, *H1′*); 8.05 (d, J = 8.1 Hz, 1H); 11.32 (bs, 1H). ^{13}C NMR (126 MHz, DMSO-d_6): δ 19.9; 57.4; 65.2; 69.1; 82.9; 85.6; 88.1; 101.8; 140.4; 150.5; 163.1. HRMS: [M + H]$^+$ calc. for $C_{11}H_{17}N_2O_6$, 273.1087; found: 273.1094.

5′-(*S*)-*C*-Methyl-2′-deoxy-2′-fluorouridine 7b. 41 mg (59%) of **7b** as an amorphous white solid was prepared analogously from compound **5b** (150 mg, 0.27 mmol). ^{1}H NMR (400 MHz, DMSO-d_6): δ 1.18 (d, J = 6.6 Hz, 3H); 3.70 (d, J = 7.1 Hz, 1H); 3.78−3.89 (m, 1H); 4.13 (dq, J = 5.1, 20.1 [^{3}*J*H-F] Hz, 1H, *H3′*); 5.00 (ddd, J = 2.3, 4.4, 53.1 [^{2}*J*H-F] Hz, 1H, *H2′*); 5.19 (d, J = 4.5 Hz, 1H, *OH*); 5.56 (d, J = 4.5 Hz, 1H, *OH*); 5.62 (d, J = 8.1 Hz, 1H); 5.91 (dd, J = 2.2, 16.7 [^{3}*J*H−F] Hz, 1H, *H1′*); 8.02 (d, J = 8.1 Hz, 1H); 11.36 (s, 1H). ^{13}C NMR (126 MHz, DMSO-d_6): δ 20.1; 64.4; 68.3; 68.4; 86.1; 86.5; 86.9; 93.7 (d, ^{1}*J*C-F = 187 Hz); 101.6; 140.3; 150.3; 163.22; 163.23. ^{19}F NMR (376 MHz, DMSO-d_6): δ −210.01 (ddd, J = 17.2, 19.7, 53.1 Hz, 1F). HRMS: [M + H]$^+$ calc. for $C_{10}H_{14}FN_2O_5$, 261.0887; found: 261.0884.

5′-(*S*)-*C*-Methyl-2′-deoxyuridine 7d. 14 mg (82%) of **7d** as an amorphous white solid was prepared analogously from compound **5d** (36 mg, 0.07 mmol). ^{1}H NMR (400 MHz, DMSO-d_6): δ 1.11 (d, J = 6.4 Hz, 3H); 1.98−2.11 (m, 2H); 3.59 (t, J = 5.1 Hz, 1H); 3.69−3.82 (m, 1H); 4.19−4.25 (m, 1H); 4.98 (d, J = 4.5 Hz, 1H, *OH*); 5.19 (d, J = 4.1 Hz, 1H, *OH*); 5.63 (dd, J = 2.1, 8.1 Hz, 1H); 6.17 (t, J = 7.2 Hz, 1H, *H1′*); 8.03 (d, J = 8.1 Hz, 1H); 11.27 (s, 1H). ^{13}C NMR (126 MHz, DMSO-d_6): δ 20.2; 55.0; 65.9; 71.3; 84.0; 90.5; 101.7; 140.6; 150.4; 163.1. HRMS: [M + H]$^+$ calc. for $C_{10}H_{15}N_2O_5$, 243.0976; found: 243.0973

5′-(*R*)-*C*-Methyl-2′-*O*-methyluridine 8a. 15 mg (69%) of **8a** as an amorphous white solid was prepared analogously from compound **6a** (45 mg, 0.08 mmol). ^{1}H NMR (400 MHz, DMSO-d_6): δ 1.09 (d, J = 6.0 Hz, 3H); 3.30 (s, 3H); 3.66 (bs, 1H); 3.72−3.82 (m, 2H); 4.22 (bs, 1H); 5.07 (d, J = 4.1 Hz, 1H); 5.11 (d, J = 4.9 Hz, 1H); 5.65 (d, J = 7.9 Hz, 1H); 5.88 (d, J = 6.4 Hz, 1H, *H1′*); 7.89 (d, J = 7.9 Hz, 1H); 11.34 (s, 1H). ^{13}C NMR (126 MHz, DMSO-d_6): δ 19.6; 57.3; 66.1; 66.9; 82.2; 85.0; 89.1; 102.1; 140.6; 150.7; 163.0. HRMS: [M + H]$^+$ calc. for $C_{11}H_{17}N_2O_6$, 273.1087; found: 273.1094.

5′-(*R*)-*C*-Methyl-2′-deoxy-2′-fluorouridine 8b. 56 mg (80%) of **8b** as an amorphous white solid was prepared analogously from compound **6b** (150 mg, 0.27 mmol). ^{1}H NMR (400 MHz, DMSO-d_6): δ 1.11 (d, J = 6.6 Hz, 3H); 3.75 (bs, 1H); 3.87−3.97 (m, 1H); 4.25 (dq, J = 5.4, 15.0 [^{3}*J*H-F] Hz, 1H, *H3′*); 5.01 (dt, J = 3.9, 53.0 [^{2}*J*H-F] Hz, 1H, *H2′*); 5.15 (d, J = 4.7 Hz, 1H, *OH*); 5.55 (d, J = 6.2 Hz, 1H, *OH*); 5.63 (d, J = 8.0 Hz, 1H); 5.94 (dd, J = 3.6, 16.0 [^{3}*J*H-F] Hz, 1H, *H1′*); 7.92 (d, J = 8.1 Hz, 1H); 11.39 (s, 1H). ^{13}C NMR (126 MHz, DMSO-d_6): δ 19.0; 65.4; 67.0; 67.1; 86.0; 86.3; 86.6; 93.2 (d, ^{1}*J*C-F = 188 Hz); 101.9; 140. 6; 150.4; 163.1. ^{19}F NMR (376 MHz, DMSO-d_6): δ −211.69 (dt, J = 15.3, 52.8 Hz, 1F). HRMS: [M + H]$^+$ calc. for $C_{10}H_{14}FN_2O_5$, 261.0887; found: 261.0884.

5′-(*R*)-*C*-Methylthymidine[49] 8c. 72 mg (91%) of **8c** as a white crystalline solid was prepared analogously from compound **6c** (170 mg, 0.31 mmol). mp (ether), 205−207 °C (decomp); mp (water) reported 205 °C.[49] ^{1}H NMR (400 MHz, DMSO-d_6): δ 1.10 (d, J = 6.5 Hz, 3H); 1.76 (d, J = 0.7 Hz, 3H); 1.94−2.08 (m, 2H); 3.55 (dd, J = 1.9, 4.2 Hz, 1H); 3.75 (dd, J = 4.4, 6.4 Hz, 1H); 4.28−4.36 (m, 1H); 4.96 (bs, 1H, *OH*); 5.15 (bs, 1H, *OH*); 6.17 (dd, J = 6.0, 8.4 Hz, 1H, *H1′*); 7.69 (d, J = 1.1 Hz, 1H); 11.26 (s, 1H). ^{13}C NMR (126 MHz, DMSO-d_6): δ 12.3; 19. 9; 56.0; 66.5; 69.5; 83.6; 90.7; 109.5; 136.2; 150.5; 163.7. HRMS: [M + H]$^+$ calc. for $C_{11}H_{17}N_2O_5$, 257.1137; found: 257.1141.

5′-(*R*)-*C*-Methyl-2′-deoxyuridine 8d. 13 mg (80%) of **8d** (dr at 5′ 97%) as an amorphous white solid was prepared analogously from compound **6d** (dr at 5′ 97%, 35 mg, 0.07 mmol). ^{1}H NMR (500 MHz, DMSO-d_6): δ 1.09 (d, J = 6.5 Hz, 3H); 1.96−2.07 (m, 2H); 3.56 (dd, J = 1.7, 4.3 Hz, 1H); 3.68−3.75 (m, 1H); 4.31 (bs, 1H); 4.92 (d, J = 5.0 Hz, 1H, *OH*); 5.17 (d, J = 4.1 Hz, 1H, *OH*); 5.62 (d, J = 8.1 Hz, 1H); 6.16 (dd, J = 6.0, 8.4 Hz, 1H); 7.82 (d, J = 8.1 Hz, 1H); 11.28 (s, 1H). ^{13}C NMR (126 MHz, DMSO-d_6): δ 19.8; 66.4; 69.5; 83.9; 90.9; 101. 9; 140. 6; 150.5; 163.1. HRMS: [M + H]$^+$ calc. for $C_{10}H_{15}N_2O_5$, 243.0976; found: 243.0974

5′-(*S*)-*C*-Methyl-5′-*O*-[bis(4-methoxyphenyl)phenylmethyl]-2′-*O*-methylcytidine 10a. TMS-Cl (0.33 mL, 2.6 mmol) was added to a stirred solution of **5a** (0.68 g, 1.2 mmol) and *N*-methyl-2-pyrrolidone (NMP, 1 mL, 10 mmol) in anhyd. CH_3CN (6 mL) under Ar atm. The mixture was stirred at r.t. for 1 h and cooled to 0 °C, and trifluoroacetic anhydride (0.42 mL, 3 mmol) was slowly added. After stirring at 0 °C for 30 min, *p*-nitrophenol (0.50 g, 3.6 mmol) was added, the mixture was stirred overnight at 0 °C, and quenched with saturated $NaHCO_3$ (25 mL), and the product was extracted into EtOAc, followed by standard workup. The residue (1.26 g) was dissolved in dioxane (12 mL), and saturated aq. NH_4OH (2 mL) was added. The mixture was heated at 60 °C in a pressure bottle overnight, cooled to r.t., and evaporated *in vacuo*. Flash chromatography of the residue over a column of silica gel with a gradient of 1−12% methanol in DCM afforded 0.55 g (81%) of pure **10a** as an amorphous white solid. ^{1}H NMR (400 MHz, acetone-d_6): δ 0.93 (d, J = 5.1 Hz, 3H); 3.48 (s, 3H); 3.64−3.72 (m, 1H); 3.77 (s, 3H); 3.78 (s, 3H); 3.80 (dd, J = 2.1, 4.4 Hz, 1H); 3.83−3.93 (m, 2H); 4.25 (t, J = 5.0 Hz, 1H); 5.92−5.97 (m, 2H); 6.88 (t split, J = 7.0 Hz, 4H); 7.13 (bs, 1H); 7.21 (t split, J = 5.8 Hz, 1H); 7.29 (t, J = 5.9 Hz, 2H); 7.39−7.47 (m, 4H); 7.52−7.57 (m, 2H); 7.86 (d, J = 6.0 Hz, 1H); 7.98 (bs, 1H). ^{13}C NMR (126 MHz, acetone-d_6): δ 18.7; 55.6; 58.7; 69.9; 70.82; 84.8; 87.4; 87.8; 88.6; 95.2; 113.8; 127.6; 128.5; 129.4; 131.46; 131.55; 137.6; 137.8; 141.7; 147.6; 156.4; 159.6; 159.7; 167.4. HRMS: [M + Na]$^+$ calc. for $C_{32}H_{35}N_3NaO_7$, 596.2373; found: 596.2380.

DOI: 10.1021/acs.joc.5b02375
J. Org. Chem. 2016, 81, 2261−2279

5′-(*R*)-*C*-Methyl-5′-*O*-[bis(4-methoxyphenyl)phenylmethyl]-2′-*O*-methylcytidine 11a. 0.39 g (85%) of **11a** as an amorphous white solid was prepared analogously from **6a** (0.46 g, 0.8 mmol). ^{1}H NMR (400 MHz, acetone-d_6): δ 0.96 (d, J = 5.2 Hz, 3H); 3.46 (s, 3H); 3.61−3.68 (m, 1H); 3.71−3.79 (m, 2H); 3.77 (s, 6H); 4.04 (bs, 1H); 4.52 (t, J = 4.6 Hz, 1H); 5.57 (d, J = 6.0 Hz, 1H); 5.98 (d, J = 3.4 Hz, 1H); 6.88 (d, J = 7.2 Hz, 4H); 7.02 (bs, 1H); 7.20 (t split, J = 5.8 Hz, 1H); 7.29 (t, J = 6.4 Hz, 2H); 7.39−7.48 (m, 5H); 7.56 (dd, J = 1.0, 6.8 Hz, 2H); 7.83 (bs, 1H). ^{13}C NMR (126 MHz, acetone-d_6): δ 18.2; 55.6; 58.7; 69.7; 70.7; 84.4; 87.5; 87.6; 88.2; 95.3; 113.8; 113.9; 127.5; 128.5; 129.2; 131.45; 131.50; 137.5; 137.6; 142.1; 147.8; 156.3; 159.67; 159.7; 167.1. HRMS: [M + Na]$^+$ calc. for $C_{32}H_{35}N_3NaO_7$, 596.2373; found: 596.2381.

5′-(*S*)-*C*-Methyl-5′-*O*-[bis(4-methoxyphenyl)phenylmethyl]-2′-deoxy-2′-fluorocytidine 10b. TMS-Cl (1.6 mL, 13 mmol) was added to a stirred solution of **5b** (1.69 g, 3 mmol) and NMP (1.6 mL, 15 mmol) in anhyd. CH_3CN (12 mL) under Ar atm. The mixture was stirred at r.t. for 1.5 h and transferred via cannula to a separately prepared and vigorously stirred mixture (2) at 0 °C under Ar atm. Preparation of mixture (2): $POCl_3$ (0.82 mL, 9 mmol) was added under Ar atm to a cooled (0 °C) and stirred suspension of 1,2,4-triazole (2.07 g, 30 mmol) in anhyd. CH_3CN (12 mL). After stirring at 0 °C for 5 min, NMP (3.4 mL, 33 mmol) was slowly added, and the transparent mixture was stirred at 0 °C for an additional 20 min before the addition of the nucleoside solution. The combined mixture was allowed to warm up to r.t. for 2 h; dioxane (24 mL) and sat. aq. NH_4OH (9 mL) were consecutively added. The mixture was stirred at r.t. overnight, the solvents were removed *in vacuum*, and the residue was partitioned between EtOAc (75 mL) and 5% aq. NaCl (75 mL), followed by a second 5% aq. NaCl wash and standard workup. Flash chromatography of the crude residue (1.80 g) over a column of silica gel with a gradient of methanol in DCM (0− 15%) afforded 1.08 g (64%) of pure **10b** as an amorphous white solid. ^{1}H NMR (400 MHz, acetone-d_6): δ 0.95 (d, J = 6.4 Hz, 3H); 3.69−3.76 (m, 1H); 3.77 (s, 3H); 3.78 (s, 3H); 3.94 (dd, J = 4.0, 8.5 Hz, 1H); 4.46 (ddd, J = 4.4, 8.4, 22.2 [^3JH-F] Hz, 1H, *H3′*); 4.62 (bs, 1H); 5.11 (ddd, J = 1.0, 4.4, 53.2 [^2JH−F] Hz, 1H, *H2′*); 5.90 (d, J = 7.4 Hz, 1H); 5.90 (dd, J = 1.0, 18.4 [^3JH-F] Hz, 1H, *H1′*); 6.87 (t split, J = 9.0 Hz, 4H); 7.03 (bs, 1H); 7.18−7.23 (m, 1H); 7.25−7.32 (m, 2H); 7.39−7.47 (m, 4H); 7.52−7.57 (m, 2H); 7.86 (d, J = 7.5 Hz, 1H). ^{13}C NMR (126 MHz, acetone-d_6): δ 18.7; 55.0; 55.57; 55.58; 66.7; 69.9; 70.4; 86.5; 87.5; 90.2; 90.5; 95.2; 95.2 (d, ^1JC-F = 186 Hz); 113.8; 127.6; 128.5; 129.4; 131.5; 131.6; 137.6; 137.9; 142.4; 147.6; 156.3; 159.6; 159.7; 167.5. ^{19}F NMR (376 MHz, acetone-d_6): δ −203.37 (ddd, J = 18.6, 22.2, 53.1 Hz, 1F). HRMS: [M + Na]$^+$ calc. for $C_{31}H_{32}FN_3NaO_6$, 584.2173; found: 584.2169.

5′-(*R*)-*C*-Methyl-5′-*O*-[bis(4-methoxyphenyl)phenylmethyl]-2′-deoxy-2′-fluorocytidine 11b (dr at 5′ ∼98%). 1.10 g (65%) of **11b** as an amorphous white solid was prepared analogously from **6b** (1.69 g, 3 mmol, dr at 5′ ∼98%). ^{1}H NMR (400 MHz, acetone-d_6): δ 0.93 (d, J = 6.6 Hz, 3H); 3.762 (s, 3H); 3.765 (s, 3H); 3.76−3.82 (m, 1H); 3.87 (dd, J = 1.9, 8.1 Hz, 1H); 4.63−4.86 (m, 2H); 5.08 (ddd, J = 1.9, 4.8, 54.2 [^2JH-F] Hz, 1H, *H2′*); 5.61 (d, J = 7.4 Hz, 1H); 5.88 (dd, J = 1.9, 20.5 [^3JH-F] Hz, 1H, *H1′*); 6.84−6.92 (m, 4H); 7.00 (bs, 1H); 7.16−7.22 (m, 1H); 7.25−7.32 (m, 2H); 7.41−7.49 (m, 4H); 7.53−7.62 (m, 3H). ^{13}C NMR (126 MHz, acetone-d_6): δ 17.5; 55.0; 55.6; 69.9; 70.1; 70.2; 85.8; 87.5; 90.3; 90.7; 94.9 (d, ^1JC-F = 186 Hz); 95.4; 113.8; 113.9; 127.5; 128.52; 129.3; 131.46; 131.47; 137.6; 137.7; 143.2; 147.7; 156.3; 159.7; 159.7; 167.4. ^{19}F NMR (376 MHz, acetone-d_6): δ −202.97 (dt, J = 20.2, 54.0 Hz, 1F). HRMS: [M + Na]$^+$ calc. for $C_{31}H_{32}FN_3NaO_6$, 584.2173; found: 584.2185.

***N*-Acetyl-5′-(*S*)-*C*-methyl-5′-*O*-[bis(4-methoxyphenyl)-phenylmethyl]-2′-*O*-methylcytidine 12a.** Acetic anhydride (0.10 mL, 1.0 mmol) was added to a stirring solution of cytidine **10a** (0.50 g, 0.87 mmol) in anhyd. DMF (3 mL) under Ar atm. The mixture was stirred overnight, cooled to 0 °C, and partitioned between 5% aq. NaCl (15 mL) and EtOAc (15 mL), followed by two successive 5% aq. NaCl wash and standard workup. The residue was coevaporated twice with CH_3CN to afford 0.51 g (96%) of **12a** as an amorphous white foam. ^{1}H NMR (500 MHz, DMSO-d_6): δ 0.78 (d, J = 6.4 Hz, 3H); 2.09 (s, 3H); 3.44 (s, 3H); 3.50−3.56 (m, 1H); 3.69−3.74 (m, 1H); 3.72 (s, 3H); 3.73 (s, 3H); 3.78−3.83 (m, 1H); 4.05−4.11 (m, 1H); 4.98 (d, J = 7.3 Hz, 1H); 5.83 (d, J = 2.8 Hz, 1H); 6.83−6.91 (m, 4H); 7.13 (d, J = 7.5 Hz, 1H); 7.18−7.23 (m, 1H); 7.34−7.36 (m, 6H); 7.39−7.46 (m, 2H); 8.12 (d, J = 7.5 Hz, 1H); 10.95 (s, 1H). ^{13}C NMR (126 MHz, DMSO-d_6): δ 20.3; 24.4; 55.0; 57.7; 64.4; 68.4; 79.9; 83.8; 78.0; 87.6; 112.8; 126.4; 127.4; 127.6; 128.9; 140.2; 148.4; 154.5; 157.8; 162.4; 171.1. HRMS: [M + H]$^+$ calc. for $C_{34}H_{38}N_3O_8$, 616.2659; found: 616.2651.

***N*-Acetyl-5′-(*S*)-*C*-methyl-5′-*O*-[bis(4-methoxyphenyl)-phenylmethyl]-2′-deoxy-2′-fluorocytidine 12b.** 1.02 g (94%) of **12b** as an amorphous white foam was prepared analogously from **10b** (1.02 g, 1.8 mmol) and acetic anhydride (0.21 mL, 2.1 mmol) in anhyd. DMF (6 mL). ^{1}H NMR (400 MHz, acetone-d_6): δ 1.00 (d, J = 6.4 Hz, 3H); 2.24 (s, 3H); 3.73−3.79 (m, 1H); 3.78 (s, 3H); 3.79 (s, 3H); 4.02 (dd, J = 4.1, 8.9 Hz, 1H); 4.37−4.50 (m, 1H); 4.53 (d, J = 7.4 Hz, 1H); 5.17 (dd, J = 4.2, 52.5 [^2JH-F] Hz, 1H, *H2′*); 5.92 (d, J = 17.6 Hz [^3JH-F], 1H, *H1′*); 6.82−6.94 (m, 4H); 7.18−7.24 (m, 1H); 7.26−7.36 (m, 3H); 7.38−7.49 (m, 4H); 7.52−7.60 (m, 2H); 8.24 (d, J = 7.6 Hz, 1H); 9.98 (s, 1H). ^{13}C NMR (126 MHz, acetone-d_6): δ 18.9; 24.9; 55.57; 55.58; 69.7; 69.8; 70.4; 87.0; 87.6; 90.7; 91.0; 95.1 (d, ^1JC-F = 186 Hz); 96.7; 113.8; 113.8; 127.6; 128.5; 131.5; 131.6; 137.4; 137.8; 145.8; 147.5; 155.6; 159.7; 159.8; 164.0; 171.6. ^{19}F NMR (376 MHz, acetone-d_6): δ −203.93 (ddd, J = 17.7, 23.6, 52.6 Hz, 1F). HRMS: [M + H]$^+$ calc. for $C_{33}H_{35}FN_3O_7$, 604.2459; found: 604.2458.

***N*-Acetyl-5′-(*R*)-*C*-methyl-5′-*O*-[bis(4-methoxyphenyl)-phenylmethyl]-2′-*O*-methylcytidine 13a.** 0.36 g (97%) of **13a** as an amorphous white foam was prepared analogously from **11a** (0.35 g, 0.61 mmol), and acetic anhydride (70 μL, 0.73 mmol) in anhyd. DMF (2 mL). ^{1}H NMR (500 MHz, DMSO-d_6): δ 0.83 (d, J = 6.5 Hz, 3H); 2.07 (s, 3H); 3.39 (s, 3H); 3.47−3.54 (m, 1H); 3.65 (dd, J = 4.3, 5.1 Hz, 1H); 3.73 (s, 6H); 3.71−3.76 (m, 1H); 4.37 (dd, J = 6.4, 12.1 Hz, 1H); 5.19 (d, J = 6.9 Hz, 1H); 5.81 (d, J = 3.9 Hz, 1H); 6.78 (d, J = 7.5 Hz, 1H); 6.85−6.92 (m, 4H); 7.20 (t, J = 7.4 Hz, 1H); 7.26−7.36 (m, 6H); 7.42−7.48 (m, 2H); 7.81 (d, J = 7.6 Hz, 1H); 10.89 (s, 1H). ^{13}C NMR (126 MHz, DMSO-d_6): δ 19.4; 24.4; 55.0; 57.6; 57.8; 65.8; 67.0; 79.9; 83.7; 87.1; 87.9; 95.6; 112.8; 126.5; 127.4; 127.6; 128.9; 140.2; 145.6; 148.4; 154.7; 157.8; 162.4; 171.1. HRMS: [M + H]$^+$ calc. for $C_{34}H_{38}N_3O_8$, 616.2659; found: 616.2654.

***N*-Acetyl-5′-(*R*)-*C*-methyl-5′-*O*-[bis(4-methoxyphenyl)-phenylmethyl]-2′-deoxy-2′-fluorocytidine 13b (dr at 5′ ∼98%).** 1.01 g (88%) of **13b** as an amorphous white foam was prepared analogously from **11b** (1.04 g, 1.9 mmol, dr at 5′ ∼98%) and acetic anhydride (0.23 mL, 2.2 mmol) in anhyd. DMF (6 mL). ^{1}H NMR (400 MHz, acetone-d_6): δ 0.99 (d, J = 6.6 Hz, 3H); 2.21 (s, 3H); 3.78 (s, 6H); 3.79−3.84 (m, 1H); 3.94 (dd, J = 2.2, 8.7 Hz, 1H); 4.71−4.84 (m, 2H); 5.14 (ddd, J = 1.2, 4.5, 53.7 [^2JH-F] Hz, 1H, *H2′*); 5.90 (dd, J = 1.2, 19.4 [^3JH-F] Hz, 1H, *H1′*); 6.84−6.93 (m, 4H); 6.98 (d, J = 7.5 Hz, 1H); 7.18−7.24 (m, 1H); 7.26−7.32 (m, 2H); 7.42−7.50 (m, 4H); 7.55−7.61 (m, 2H); 8.03 (d, J = 7.6 Hz, 1H); 9.94 (s, 1H). ^{13}C NMR (100 MHz, acetone-d_6): δ 17.7; 24.9; 55.55; 55.56; 69.7; 69.9; 70.0; 85.9; 87.6; 90.6; 90.1; 95.0 (d, ^1JC-F = 186 Hz); 96.8; 113.9; 113.94; 127.6; 128.6; 129.2; 131.3; 131.5; 137.3; 137.9; 146.47; 147.49; 155.6; 159.69; 159.73; 164.0; 171.4. ^{19}F NMR (376 MHz, acetone-d_6): δ −203.26 (dt, J = 20.0, 53.3 Hz, 1F). HRMS: [M + H]$^+$ calc. for $C_{33}H_{35}FN_3O_7$, 604.2459; found: 604.2466.

5′-(*S*)-*C*-Methyl-5′-*O*-[bis(4-methoxyphenyl)phenylmethyl]-2′-*O*-methyl-3′-[2-cyanoethyl-*N*,*N*-bis(1-methylethyl)phosphoramidite]-uridine 14a. DIEA (0.92 mL, 5.3 mmol) and 2-cyanoethyl *N*,*N*-diisopropylchlorophosphoramidite (1.20 mL, 5.3 mmol) were added consecutively to a stirred solution of compound **5a** (2.00 g, 3.5 mmol) in anhyd. DCM (20 mL) under Ar atm. After stirring at r.t. for 3 h, the mixture was quenched by addition of saturated aq. $NaHCO_3$, and the product was extracted into EtOAc (80 mL), followed by standard workup. Flash chromatography of the residue over a column of silica gel with a gradient of 50−90% EtOAc in hexanes containing 0.5% of TEA yielded 2.47 g (91%) of **14a** as a colorless amorphous foam; phosphorus diastereomer ratio: ∼0.57:0.43. ^{1}H NMR (400 MHz, CD_3OD): δ 0.90 (d, J = 6.4 Hz, 1.7H); 0.97 (d, J = 6.4 Hz, 1.3H); 1.05 (d, J = 6.8 Hz, 3.3H); 1.11−

DOI: 10.1021/acs.joc.5b02375
J. Org. Chem. 2016, 81, 2261−2279

1.18 (m, 8.7H); 2.30−2.45 (m, 0.9H); 2.65 (t, J = 6.1 Hz, 1.1H); 3.38 (s, 1.3H); 3.44 (s, 1.7H); 3.50−3.66 (m, 4H); 3.68−3.84 (m, 7H); 3.95 (t, J = 3.6 Hz, 1H); 3.98 (dt, J = 0.9, 5.0 Hz, 1H); 4.24−4.34 (m, 1H); 5.57 (d, J = 8.1 Hz, 0.57H); 5.60 (d, J = 8.0 Hz, 0.43H); 5.88 (d, J = 5.1 Hz, 0.57H); 5.89 (d, J = 4.9 Hz, 0.43H); 6.84−6.91 (m, 4H); 7.20−7.26 (m, 1H); 7.27−7.33 (m, 2H); 7.33−7.42 (m, 4H); 7.45−7.50 (m, 2H); 7.81 (d, J = 8.2 Hz, 0.57H); 7.92 (d, J = 8.2 Hz, 0.43H); 9.23 (bs, 1H). ^{31}P NMR (162 MHz, CD_3OD): δ 154.98; 155.33. HRMS: $[M + H]^+$ calc. for $C_{41}H_{52}N_4O_9P$, 775.3472; found: 775.3507.

5′-(*S*)-*C*-Methyl-5′-*O*-[bis(4-methoxyphenyl)phenylmethyl]-2′-deoxy-2′-fluoro-3′-[2-cyanoethyl-*N*,*N*-bis(1-methylethyl)-phosphoramidite]-uridine 14b. 4.28 g (89%) of **14b** as a colorless amorphous foam with a phosphorus diastereomer ratio ∼ 0.54:0.46 was prepared analogously from **5b** (3.53 g, 6.3 mmol) and 2-cyanoethyl *N*,*N*-diisopropylchlorophosphoramidite (2.10 mL, 9.5 mmol) in the presence of DIEA (1.70 mL, 9.5 mmol) in DCM (30 mL). ^{1}H NMR (400 MHz, CD_3OD): δ 0.93 (d, J = 6.4 Hz, 1.4H); 0.99 (d, J = 6.4 Hz, 1.6H); 1.09 (d, J = 6.8 Hz, 3H); 1.10 (d, J = 6.8 Hz, 3H); 1.15 (t, J = 6.6 Hz, 6H); 2.39 (t, J = 6.0 Hz, 1.1H); 2.61 (t, J = 6.3 Hz, 0.9H); 3.52−3.70 (m, 4.5H); 3.72−3.80 (m, 6.5H); 3.94 (dt, J = 3.6, 8.5 Hz, 1H); 4.40−4.60 (m, 1H); 5.14 (ddd, J = 1.2, 4.6, 52.2 [^2JH−F] Hz, 0.46H, *H2′*); 5.22 (ddd, J = 1.8, 4.6, 52.6 [^2JH-F] Hz, 0.54H, *H2′*); 4.46 (d, J = 8.1 Hz, 0.46H); 5.52 (d, J = 8.2 Hz, 0.54H); 5.84 (dd, J = 1.3, 18.4 [^3JH-F] Hz, 0.46H, *H1′*); 5.86 (dd, J = 1.8, 18.0 [^3JH-F] Hz, 0.54H, *H1′*); 6.82−6.90 (m, 4H); 7.19−7.25 (m, 1H); 7.26−7.32 (m, 2H); 7.32−7.42 (m, 4H); 7.45−7.50 (m, 2H); 7.77 (d, J = 8.2 Hz, 0.46H); 7.83 (d, J = 8.2 Hz, 0.54H); 9.26 (bs, 1H). ^{19}F NMR (376 MHz, CD_3OD): δ −200.94 to −201.27 (m, 0.46F); −202.15 to −202.48 (m, 0.54F).^{31}P NMR (162 MHz, CD_3OD): δ 155.05 (d, J = 14.8 Hz, 0.54P); 155.61 (d, J = 8.6 Hz, 0.46P). HRMS: $[M + H]^+$ calc. for $C_{40}H_{49}FN_4O_8P$, 763.3272; found: 763.3276.

5′-(*S*)-*C*-Methyl-5′-*O*-[bis(4-methoxyphenyl)phenylmethyl]-3′-[2-cyanoethyl-*N*,*N*-bis(1-methylethyl)phosphoramidite]-thymidine 14c. 5.12 g (90%) of **14c** as a colorless amorphous foam with a phosphorus diastereomer ratio ∼ 0.6:0.4 was prepared analogously from **5c** (4.20 g, 7.5 mmol) and 2-cyanoethyl *N*,*N*-diisopropylchlorophosphoramidite (2.50 mL, 11 mmol) in the presence of DIEA (1.90 mL, 11 mmol) in DCM (30 mL). ^{1}H NMR (500 MHz, CD_3OD): δ 0.86 (d, J = 6.4 Hz, 1.2H); 0.91 (d, J = 6.4 Hz, 1.8H); 1.07 (d, J = 6.8 Hz, 2.4H); 1.14 (d, J = 6.7 Hz, 4.8H); 1.16 (d, J = 6.9 Hz, 4.8H); 1.73 (s split, 3H); 2.21−2.29 (m, 1H); 2.36 (ddd, J = 2.8, 5.6, 13.5 Hz, 0.6H); 2.39−2.44 (m, 0.4H); 2.46 (t, J = 6.2 Hz, 0.6H); 2.47 (t, J = 6.0 Hz, 0.6H); 2.63 (t, J = 5.9 Hz, 0.8H); 3.53−3.72 (m, 4.4H); 3.74−3.82 (m, 7H); 3.83 (t, J = 3.4 Hz, 0.6H); 4.51−4.57 (m, 1H); 6.12−6.17 (m, 1H); 6.83−6.89 (m, 4H); 7.19−7.24 (m, 1H); 7.25−7.32 (m, 2H); 7.35−7.43 (m, 4H); 7.48−7.53 (m, 2H); 7.57 (d, J = 1.3 Hz, 0.4H); 7.63 (d, J = 1.3 Hz, 0.6H); 9.33 (bs, 1H). ^{31}P NMR (202 MHz, CD_3OD): δ 149.63; 149.97. HRMS: $[M + Na]^+$ calc. for $C_{41}H_{51}N_4NaO_8P$, 781.3342; found: 781.3376.

5′-(*S*)-*C*-Methyl-5′-*O*-[bis(4-methoxyphenyl)phenylmethyl]-2′-deoxy-3′-[2-cyanoethyl-*N*,*N*-bis(1-methylethyl)phosphoramidite]-uridine 14d. 2.98 g (87%) of **14d** as a colorless amorphous foam with a phosphorus diastereomer ratio ∼ 0.5:0.5 was prepared analogously from **5d** (2.51 g, 4.6 mmol) and 2-cyanoethyl *N*,*N*-diisopropylchlorophosphoramidite (1.54 mL, 6.9 mmol) in the presence of DIEA (1.20 mL, 6.9 mmol) in DCM (20 mL). ^{1}H NMR (500 MHz, DMSO-d_6): δ 0.65 (d, J = 6.2 Hz, 1.5H); 0.72 (d, J = 6.3 Hz, 1.5H); 0.94 (d, J = 6.4 Hz, 1.5H); 1.06 (d, J = 6.8 Hz, 3H); 1.09−1.16 (m, 7.5H); 2.14−2.43 (m, 2H); 2.57−2.69 (m, 1H); 2.77 (t, J = 5.8 Hz, 1H); 3.38−3.50 (m, 0.5H); 3.51−3.60 (m, 2.5H); 3.60−3.69 (m, 2.5H); 3.71−3.75 (m, 6H); 3.75−3.81 (m, 1.5H); 4.47−4.58 (m, 1H); 5.59 (d, J = 8.1 Hz, 1H); 5.98−6.05 (m, 1H); 6.82−6.92 (m, 4H); 7.17−7.24 (m, 1H); 7.24−7.34 (m, 6H); 7.40−7.45 (m, 2H); 7.59 (d, J = 8.2 Hz, 0.5H); 7.63 (d, J = 8.1 Hz, 0.5H); 11.35 (bs, 1H). ^{31}P NMR (126 MHz, DMSO-d_6): δ 148.44; 149.24. HRMS: $[M + Na]^+$ calc. for $C_{40}H_{49}N_4NaO_8P$, 767.3186; found: 767.3215.

5′-(*R*)-*C*-Methyl-5′-*O*-[bis(4-methoxyphenyl)phenylmethyl]-2′-*O*-methyl-3′-[2-cyanoethyl-*N*,*N*-bis(1-methylethyl)phosphoramidite]-uridine 15a. 1.21 g (92%) of **15a** as a colorless amorphous foam with a phosphorus diastereomer ratio ∼ 0.56:0.44 was prepared analogously from **6a** (1.00 g, 1.7 mmol) and 2-cyanoethyl *N*,*N*-diisopropylchlorophosphoramidite (0.58 mL, 2.6 mmol) in the presence of DIEA (0.45 mL, 2.6 mmol) in DCM (10 mL). ^{1}H NMR (400 MHz, CD_3OD): δ 0.926 (d, J = 6.6 Hz, 1.7H); 0.931 (d, J = 6.6 Hz, 1.3H); 1.15−1.25 (m, 12H); 2.60−2.65 (m, 0.9H); 2.65 (t, J = 6.9 Hz, 1.1H); 3.42 (s, 1.3H); 3.45 (s, 1.7H); 3.48−3.56 (m, 1H); 3.61−3.74 (m, 2.3H); 3.74−3.84 (m, 1.7H); 3.764 (s, 3.4H); 3.768 (s, 2.6H); 3.84−3.95 (m, 1.6H); 3.97 (dd, J = 2.9, 4.4 Hz, 0.4H); 4.60 (dt, J = 5.3, 10.0 Hz, 0.56H); 4.69 (dt, J = 5.0, 9.8 Hz, 0.44H); 5.08 (d, J = 8.1 Hz, 1H); 5.77 (d, J = 4.6 Hz, 0.56H); 5.79 (d, J = 5.2 Hz, 0.44H); 6.84−6.92 (m, 4H); 7.20−7.34 (m, 4H); 7.37−7.47 (m, 4H); 7.50−7.56 (m, 2H); 9.23 (bs, 1H). ^{31}P NMR (162 MHz, CD_3OD): δ 154.24; 154.97. HRMS: $[M + H]^+$ calc. for $C_{41}H_{52}N_4O_9P$, 775.3472; found: 775.3488.

5′-(*R*)-*C*-Methyl-5′-*O*-[bis(4-methoxyphenyl)phenylmethyl]-2′-deoxy-2′-fluoro-3′-[2-cyanoethyl-*N*,*N*-bis(1-methylethyl)-phosphoramidite]-uridine 15b. 2.71 g (89%) of **15b** as a colorless amorphous foam with a phosphorus diastereomer ratio ∼ 0.6:0.4 was prepared analogously from **6b** (2.28 g, 4.0 mmol) and 2-cyanoethyl *N*,*N*-diisopropylchlorophosphoramidite (1.30 mL, 6.0 mmol) in the presence of DIEA (1.10 mL, 6.0 mmol) in DCM (20 mL). ^{1}H NMR (400 MHz, CD_3OD): δ 0.87 (d, J = 6.6 Hz, 1.2H); 0.88 (d, J = 6.6 Hz, 1.8H); 1.14 (d, J = 6.8 Hz, 3.6H); 1.17 (d, J = 6.8 Hz, 2.4H); 1.20 (d, J = 6.7 Hz, 3.6H); 1.21 (d, J = 6.7 Hz, 2.4H); 2.60 (t, J = 5.9 Hz, 0.8H); 2.69 (t, J = 5.9 Hz, 1.2H); 3.57−3.69 (m, 2H); 3.69−3.82 (m, 2.4H); 3.76 (s, 3.6H); 3.77 (s, 2.4H); 3.86−3.95 (m, 1.6H); 4.59−4.78 (m, 1H); 5.07−5.12 (m, 0.5H); 5.15 (d, J = 8.1 Hz, 0.6H); 5.19 (d, J = 8.1 Hz, 0.4H); 5.21−5.25 (m, 0.5H); 5.74 (d, J = 21.2 [^3JH-F] Hz, 0.6H, *H1′*); 5.76 (dd, J = 1.8, 20.3 [^3JH-F] Hz, 0.4H, *H1′*); 6.83−6.91 (m, 4H); 7.19−7.25 (m, 1H); 7.26−7.33 (m, 2H); 7.36−7.46 (m, 5H); 7.49−7.55 (m, 2H); 9.17 (bs, 1H). ^{19}F NMR (376 MHz, CD_3CN): δ −199.45, −199.89 (m, 0.6F); −201.27 to −201.65 (m, 0.4F).^{31}P NMR (162 MHz, CD_3CN): δ 154.87 (d, J = 10.0 Hz, 0.6P); 155.04 (d, J = 10.8 Hz, 0.4P). HRMS: $[M + H]^+$ calc. for $C_{40}H_{49}FN_4O_8P$, 763.3272; found: 763.3254.

5′-(*R*)-*C*-Methyl-5′-*O*-[bis(4-methoxyphenyl)phenylmethyl]-3′-[2-cyanoethyl-*N*,*N*-bis(1-methylethyl)phosphoramidite]-thymidine 15c. 2.21 g (91%) of **15c** as a colorless amorphous foam with a phosphorus diastereomer ratio ∼ 0.54:0.46 was prepared analogously from **6c** (1.80 g, 3.2 mmol) and 2-cyanoethyl *N*,*N*-diisopropylchlorophosphoramidite (1.10 mL, 4.8 mmol) in the presence of DIEA (0.83 mL, 4.8 mmol) in DCM (15 mL). ^{1}H NMR (400 MHz, CD_3CN): δ 0.86 (d, J = 6.4 Hz, 1.4H); 0.89 (d, J = 6.4 Hz, 1.6H); 1.12−1.24 (m, 12H); 1.46 (d, J = 1.1 Hz, 1.6H); 1.48 (d, J = 1.1 Hz, 1.4H); 2.06−2.17 (m, 1H); 2.28 (ddd, J = 1.7, 5.7, 13.8 Hz, 0.54H); 2.35 (ddd, J = 2.5, 6.0, 13.8 Hz, 0.46H); 2.62 (dt, J = 2.4, 6.1 Hz, 1.1H); 2.66 (t, J = 5.9 Hz, 0.9H); 3.41−3.50 (m, 1H); 3.54−3.69 (m, 2H); 3.69−3.80 (m, 7.5H); 3.80−3.88 (m, 1H); 3.90 (t, J = 3.3 Hz, 0.5H); 4.76−4.85 (m, 1H); 6.13−6.20 (m, 1H); 6.81−6.90 (m, 4H); 7.02 (s split, 1H); 7.17−7.24 (m, 1H); 7.25−7.32 (m, 2H); 7.37−7.45 (m, 4H); 7.50−7.56 (m, 2H); 9.33 (bs, 1H). ^{31}P NMR (202 MHz, CD_3CN): δ 149.04; 149.42. HRMS: $[M + Na]^+$ calc. for $C_{41}H_{51}N_4NaO_8P$, 781.3342; found: 781.3357.

5′-(*R*)-*C*-Methyl-5′-*O*-[bis(4-methoxyphenyl)phenylmethyl]-2′-deoxy-3′-[2-cyanoethyl-*N*,*N*-bis(1-methylethyl)phosphoramidite]-uridine 15d. 1.70 g (80%) of **15d** as a colorless amorphous foam with a phosphorus diastereomer ratio ∼ 0.5:0.5 was prepared analogously from **6d** (1.55 g, 2.8 mmol) and 2-cyanoethyl *N*,*N*-diisopropylchlorophosphoramidite (0.94 mL, 4.2 mmol) in the presence of DIEA (0.73 mL, 4.2 mmol) in DCM (10 mL). ^{1}H NMR (400 MHz, DMSO-d_6): δ 0.74 (d, J = 6.4 Hz, 1.5H); 0.77 (d, J = 6.4 Hz, 1.5H); 1.07 (d, J = 6.7 Hz, 3H); 1.09−1.18 (m, 9H); 2.04−2.32 (m, 2H); 2.70 (dt, J = 1.4, 5.4 Hz, 1H); 2.77 (t, J = 6.0 Hz, 1H); 3.45−3.61 (m, 3H); 3.61−3.82 (m, 2.5H); 3.73 (s, 6H); 3.84 (t, J = 3.3 Hz, 0.5H); 4.54−4.64 (m, 1H); 5.25 (d, J = 8.2 Hz, 0.5H); 5.28 (d, J = 8.2 Hz, 0.5H); 6.05 (d, J = 7.3 Hz, 0.5H); 6.07 (d, J = 6.2 Hz, 0.5H); 6.84−6.92 (m, 4H); 7.17−7.24 (m, 1H); 7.25−7.35 (m, 7H); 7.40−7.46 (m, 2H); 11.3 (bs, 1H). ^{31}P NMR (162 MHz, DMSO-d_6): δ 149.04; 149.42. HRMS: $[M + Na]^+$ calc. for $C_{40}H_{49}N_4NaO_8P$, 767.3186; found: 767.3218.

DOI: 10.1021/acs.joc.5b02375
J. Org. Chem. 2016, 81, 2261−2279

5′-(*S*)-*C*-Methyl-*N*-acetyl-5′-*O*-[bis(4-methoxyphenyl)-phenylmethyl]-2′-*O*-methyl-3′-[2-cyanoethyl-*N*,*N*-bis(1-methylethyl)phosphoramidite]-cytidine 16a. 0.61 g (92%), of **16a** as a colorless amorphous foam with a phosphorus diastereomer ratio ∼ 0.5:0.5 was prepared analogously from **12a** (0.50 g, 0.81 mmol) and 2-cyanoethyl *N*,*N*-diisopropylchlorophosphoramidite (0.27 mL, 1.2 mmol) in the presence of DIEA (0.21 mL, 1.2 mmol) in DCM (5 mL). ^{1}H NMR (400 MHz, CD_3CN): δ 0.94 (d, J = 6.4 Hz, 1.5H); 1.01 (d, J = 6.5 Hz, 1.5H); 1.05 (d, J = 6.8 Hz, 3H); 1.08 (d, J = 6.8 Hz, 3H); 1.12 (d, J = 6.8 Hz, 3H); 1.13 (d, J = 6.8 Hz, 3H); 2.13 (s, 1.5H); 2.14 (s, 1.5H); 2.33 (t, J = 6.1 Hz, 1H); 2.60 (t, J = 5.9 Hz, 1H); 3.45−3.75 (m, 5H); 3.51 (s, 1.5H); 3.54 (s, 1.5H); 3.759 (s, 1.5H); 3.762 (s, 1.5H); 3.770 (s, 1.5H); 3.773 (s, 1.5H); 3.93 (dd, J = 2.5, 4.9 Hz, 0.5H); 3.96−4.18 (m, 1.5H); 4.25−4.38 (m, 1H); 5.90 (d, J = 2.5 Hz, 0.5H); 5.93 (d, J = 2.2 Hz, 0.5H); 6.82−6.91 (m, 4H); 7.08 (d, J = 7.5 Hz, 0.5H); 7.13 (d, J = 7.5 Hz, 0.5H); 7.20−7.42 (m, 7H); 7.44−7.50 (m, 2H); 8.28 (d, J = 7.5 Hz, 0.5H); 8.50 (d, J = 7.5 Hz, 0.5H); 9.12 (s, 1H). ^{31}P NMR (162 MHz, CD_3CN): δ 154.56; 154.99. HRMS: $[M + H]^+$ calc. for $C_{43}H_{55}N_5O_9P$, 816.3737; found: 816.3711.

5′-(*S*)-*C*-Methyl-*N*-acetyl-5′-*O*-[bis(4-methoxyphenyl)-phenylmethyl]-2′-deoxy-2′-fluoro-3′-[2-cyanoethyl-*N*,*N*-bis(1-methylethyl)phosphoramidite]-cytidine 16b. 1.01 g (96%) of **16b** as a colorless amorphous foam with a phosphorus diastereomer ratio ∼ 0.57:0.43 was prepared analogously from **12b** (0.77 g, 1.3 mmol) and 2-cyanoethyl *N*,*N*-diisopropylchlorophosphoramidite (0.45 mL, 2.0 mmol) in the presence of DIEA (0.35 mL, 2.0 mmol) in DCM (8 mL). ^{1}H NMR (400 MHz, CD_3CN): δ 0.97 (d, J = 6.4 Hz, 1.3H); 1.03 (d, J = 6.5 Hz, 1.7H); 1.07 (d, J = 6.8 Hz, 3.4H); 1.08 (d, J = 6.8 Hz, 2.6H); 1.13 (d, J = 6.6 Hz, 2.6H); 1.14 (d, J = 6.7 Hz, 3.4H); 2.14 (s, 1.3H); 2.15 (s, 1.7H); 2.36 (t, J = 6.0 Hz, 1.1H); 2.58 (dt, J = 1.6, 5.8 Hz, 0.9H); 3.47−3.73 (m, 5H); 3.752 (s, 1.3H); 3.757 (s, 1.7H); 3.763 (s, 1.3H); 3.768 (s, 1.7H); 3.99−4.07 (m, 1H); 4.38−4.59 (m, 1H); 5.13 (dd, J = 4.3, 51.8 [^2JH−F] Hz, 0.43H, *H2′*); 5.25 (dd, J = 4.2, 52.2 [^2JH−F] Hz, 0.57H, *H2′*); 5.91 (d, J = 18.2 [^3JH−F] Hz, 0.43H, *H1′*); 5.93 (d, J = 17.9 [^3JH−F] Hz, 0.57H, *H1′*); 6.80−6.89 (m, 4H); 7.10 (d, J = 7.5 Hz, 0.43H); 7.15 (d, J = 7.5 Hz, 0.57H); 7.19−7.41 (m, 7H); 7.44−7.49 (m, 2H); 8.26 (d, J = 7.5 Hz, 0.43H); 8.42 (d, J = 7.6 Hz, 0.57H); 9.35 (s, 1H). ^{19}F NMR (376 MHz, CD_3CN): δ −204.77 to −205.17 (m, 0.43F); −205.87 to −206.28 (m, 0.57F).^{31}P NMR (162 MHz, CD_3CN): δ 150.67 (d, J = 13.4 Hz, 0.57P); 151.55 (d, J = 7.2 Hz, 0.43P). HRMS: $[M + H]^+$ calc. for $C_{42}H_{52}FN_5O_8P$, 804.3538; found: 804.3554.

5′-(*R*)-*C*-Methyl-*N*-acetyl-5′-*O*-[bis(4-methoxyphenyl)-phenylmethyl]-2′-*O*-methyl-3′-[2-cyanoethyl-*N*,*N*-bis(1-methylethyl)phosphoramidite]-cytidine 17a. 0.40 g (87%) of **17a** as a colorless amorphous foam with a phosphorus diastereomer ratio ∼ 0.55:0.45 was prepared analogously from **13a** (0.35 g, 0.57 mmol) and 2-cyanoethyl *N*,*N*-diisopropylchlorophosphoramidite (0.19 mL, 0.86 mmol) in the presence of DIEA (0.15 mL, 0.86 mmol) in DCM (4 mL). ^{1}H NMR (400 MHz, CD_3CN): δ 0.95 (d, J = 6.7 Hz, 3H); 1.15−1.25 (m, 12H); 2.11 (s, 3H); 2.63 (t, J = 5.6 Hz, 0.9H); 2.67 (t, J = 6.0 Hz, 1.1H); 3.50 (s split, 1.4H); 3.52 (s split, 1.6H); 3.55−3.73 (m, 3H); 3.74−3.80 (m, 7H); 3.80−3.92 (m, 2H); 3.95 (dd, J = 1.8, 7.4 Hz, 0.55H); 4.00 (dd, J = 1.9, 7.1 Hz, 0.45H); 4.58−4.66 (m, 0.55H); 4.69−4.76 (m, 0.45H); 5.79 (d, J = 2.5 Hz, 0.55H); 5.83 (d, J = 3.0 Hz, 0.45H); 6.747 (d, J = 7.5 Hz, 0.55H); 6.751 (d, J = 7.5 Hz, 0.45H); 6.82−6.91 (m, 4H); 7.18−7.25 (m, 1H); 7.25−7.33 (m, 2H); 7.38−7.48 (m, 4H); 7.55 (t split, J = 8.2 Hz, 2H); 7.87 (d, J = 7.5 Hz, 1H); 9.09 (bs, 1H). ^{31}P NMR (162 MHz, CD_3CN): δ 154.35; 154.42. HRMS: $[M + H]^+$ calc. for $C_{43}H_{55}N_5O_9P$, 816.3737; found: 816.3738.

5′-(*R*)-*C*-Methyl-*N*-acetyl-5′-*O*-[bis(4-methoxyphenyl)-phenylmethyl]-2′-deoxy-2′-fluoro-3′-[2-cyanoethyl-*N*,*N*-bis(1-methylethyl)phosphoramidite]-cytidine 17b. 0.98 g (94%) of **17b** as a colorless amorphous foam, dr at 5′ ∼98%, with a phosphorus diastereomer ratio ∼ 0.5:0.5 was prepared analogously from **13b** (0.76 g, 1.3 mmol, dr at 5′ ∼98%) and 2-cyanoethyl *N*,*N*-diisopropyl-chlorophosphoramidite (0.45 mL, 2.0 mmol) in the presence of DIEA (0.35 mL, 2.0 mmol) in DCM (8 mL). ^{1}H NMR (400 MHz, CD_3CN): δ 0.91 (d, J = 6.7 Hz, 1.5H); 0.92 (d, J = 6.7 Hz, 1.5H); 1.16 (d, J = 6.8 Hz, 3H); 1.17 (d, J = 6.8 Hz, 3H); 1.19−1.24 (m, 6H); 2.121 (s, 1.5H); 2.125 (s, 1.5H); 2.61 (t, J = 5.9 Hz, 1H); 2.68 (t, J = 5.9 Hz, 1H); 3.59−3.94 (m, 11H); 3.96 (d, J = 9.5 Hz, 0.5H); 4.01 (d, J = 9.2 Hz, 0.5H); 4.67−4.86 (m, 1H); 5.15 (dd, J = 4.5, 52.7 [^2JH-F] Hz, 0.5H, *H2′*); 5.19 (dd, J = 4.5, 53.0 [^2JH-F] Hz, 0.5H, *H2′*); 5.793 (d, J = 20.6 [^3JH-F] Hz, 0.5H, *H1′*)); 5.796 (d, J = 20.2 [^3JH-F] Hz, 0.5H, *H1′*); 6.80−6.91 (m, 5H); 7.18−7.24 (m, 1H); 7.25−7.32 (m, 2H); 7.37−7.47 (m, 4H); 7.50−7.57 (m, 2H); 7.92 (d, J = 7.5 Hz, 0.5H); 7.94 (d, J = 7.4 Hz, 0.5H); 9.30 (bs, 1H). ^{19}F NMR (376 MHz, CD_3CN): δ −203.53 to −203.94 (m, 0.5F); −204.54 to −205.05 (m, 0.5F). ^{31}P NMR (162 MHz, CD_3CN): δ 150.61 (d, J = 9.9 Hz, 0.5P); 150.79 (d, J = 8.2 Hz, 0.5P). HRMS: $[M + H]^+$ calc. for $C_{42}H_{52}FN_5O_8P$, 804.3538; found: 804.3522.

CPG-Support 18a. A solution of **5a** (100 mg, 0.17 mmol), succinic anhydride (50 mg, 0.50 mmol), and DMAP (61 mg, 0.50 mmol) in anhyd. pyridine (3 mL) was stirred at r.t. under Ar atm for 25 h. The mixture was diluted with EtOAc (25 mL) and quenched by addition of 20 mL of 5% aq. NaCl containing 5% of phosphoric acid. The organic phase was separated and washed consecutively with 5% aq. NaCl, followed by standard workup. The residue was coevaporated once with anhyd. CH_3CN, the flask was filled with Ar, and HBTU (68 mg, 0.18 mmol), anhyd. DMF (6 mL), and DIEA (0.1 mL, 0.5 mmol) were consecutively added. After gentle shaking for ∼5 min, CPG (585 Å, maximum capacity: 124 μmol/g, 1.60 g, 0.2 mmol) was added. After shaking for 3 h, the mixture was filtered, the residue was washed consecutively with DCM, 20% methanol in DCM, DCM twice, and dried in vacuum to afford 1.55 g of precapped support. The latter was treated under Ar atm with anhyd. pyridine (8 mL) and acetic anhydride (0.8 mL). After gentle shaking for 1 h, the solids were filtered, washed twice with DCM, once with 20% MeOH in DCM, again twice with DCM, and dried under high vacuum for 1 h to afford support **18a** (1.51 g), loading: 61 μmol/g.

CPG-Support 18b. 4.48 g of **18b** with 61 μmol/g loading was prepared analogously from **5b** (282 mg, 0.5 mmol) and CPG (585 Å, maximum capacity: 124 μmol/g, 4.50 g, 0.56 mmol).

CPG-Support 19a. Was prepared analogously from **6a** (100 mg, 0.17 mmol) and CPG-585 (maximum capacity: 124 μmol/g) (1.60 g, 0.2 mmol). Obtained: 1.57 g of **18b**, loading: 60 mmol/g.

CPG-Support 19b. Was prepared analogously from **6b** (282 mg, 0.5 mmol) and CPG-585 (maximum capacity: 124 μmol/g) (4.50 g, 0.56 mmol). Obtained: 4.56 g of **19b**, loading: 51 mmol/g.

CPG-Support 20b. Was prepared analogously from **12b** (201 mg, 0.33 mmol) and CPG-585 (maximum capacity: 124 μmol/g) (2.90 g, 0.36 mmol). Obtained: 2.84 g of **20b**, loading: 62 mmol/g.

CPG-Support 21b. Was prepared analogously from **13b** (202 mg, 0.33 mmol) and CPG-585 (maximum capacity: 124 μmol/g) (2.90 g, 0.36 mmol). Obtained: 2.86 g of **20b**, loading: 64 mmol/g.

Synthesis of Oligonucleotides and T_m Measurements. Oligonucleotides were synthesized, purified, and analyzed on an ABI-394 synthesizer by following reported procedures.[6] Thermal melting temperatures of the duplexes were determined as described in the literature.[53]

SVPD Stability Measurements and Graphs. DNA single strand solutions were prepared at 0.1 mg/mL concentration in 50 mM TRIS-HCl buffer (pH 8), containing 10 mM $MgCl_2$. 1 mU/mL snake venom phosphodiesterase I (Sigma-Aldrich) was added to the DNA mixture prior to first injection, and enzymatic degradation kinetics were monitored for 24 h at r.t. Time points (0−24 h) were injected directly on the analytical HPLC ion-exchange column (one time point injection every 1 h) from the same sample preparation and analyzed by using a Dionex DNAPac PA200 analytical column at 30 °C column temperature. A gradient of 37−52% 1 M NaBr, 10% CH_3CN, 20 mM sodium phosphate buffer at pH 11, over 10 min with a flow rate of 1 mL/min was used to analyze each sample. Peak integration at 260 nm was used to calculate percentage of enzymatic degradation for each time point, as normalized per the area of the sample at time 0 h. Decay curves were plotted using XLFit in Microsoft Excel. Half-lives were determined at the time corresponding to 50% of total normalized integration area (50% of degradation). The enzymatic degradation method was calibrated at each run for a standard enzyme control oligonucleotide: dTdTdTdTdTdTdTdTdTdTdTdTdTdTdT-

DOI: 10.1021/acs.joc.5b02375
J. Org. Chem. 2016, 81, 2261−2279

dTdT●dT, where ● represents a phosphorothioate (PS) linkage and dT is 2′-deoxythymidine nucleotide; with the half-life of the enzyme control oligonucleotide being 2.5 h ± 0.3h. Each degradation experiment was run in duplicate. Representative decay curves and HPLC plots are shown in the SI.

■ ASSOCIATED CONTENT

Supporting Information

The Supporting Information is available free of charge on the ACS Publications website at DOI: 10.1021/acs.joc.5b02375.

NMR spectra; X-ray crystal structures of compounds **1a**, **1d**, **3c**, **3d**, **4a**, **4c**, **7c**, and **8c**, and time-course HPLC profile of SVPD digestion of poly(dT) containing 5′-methylated pyrimidines at the 3′-end. Cambridge Crystallographic Data Centre file numbers: CCDC 1435399 (**1b**), CCDC 1435400 (**1d**), CCDC 1435401 (**4a**), CCDC 1435402 (**4b**), CCDC 1435403 (**4c**), CCDC 1435404 (**1a**), CCDC 1435405 (**3b**), CCDC 1435406 (**3c**), CCDC 1435407 (**3d**), CCDC 1435408 (**7c**), and CCDC 1435409 (**8c**) (PDF)

■ AUTHOR INFORMATION

Corresponding Authors

*E-mail: rajeevk@alnylam.com (K.G.R.).

*E-mail: mmanoharan@alnylam.com (M.M.).

Author Contributions

The manuscript was written through contributions of all authors, and all have given approval to the final version of the manuscript.

Notes

The authors declare the following competing financial interest(s): All Alnylam Pharmaceuticals authors except R.M.M. are current employees with salary and stock options.

■ ACKNOWLEDGMENTS

We thank Professor Michael E. Jung for valuable advice and discussions. Vanderbilt University is a member institution of the Life Sciences Collaborative Access Team at Sector 21 of the Advanced Photon Source, Argonne, IL. Use of the Advanced Photon Source at Argonne National Laboratory was supported by the United States Department of Energy, Office of Science, Office of Basic Energy Sciences, under Contract DE-AC02-06CH11357.

■ REFERENCES

(1) Lieberman, J.; Sharp, P. A. *JAMA, J. Am. Med. Assoc.* **2015**, *313*, 1207.

(2) Joshi, B. H.; Pachchigar, K. P. *Biotechnol. Genet. Eng. Rev.* **2014**, *30*, 1.

(3) Wu, S. Y.; Lopez-Berestein, G.; Calin, G. A.; Sood, A. K. *Sci. Transl. Med.* **2014**, *6*, 240ps7.

(4) http://www.alnylam.com/capella/presentations/12-month-clinical-data-from-patisiran-phase-2-open-label-extension-ole-study/.

(5) http://www.alnylam.com/capella/presentations/aln-at3-isth-june2015/.

(6) Nair, J. K.; Willoughby, J. L. S.; Chan, A.; Charisse, K.; Alam, M. R.; Wang, Q.; Hoekstra, M.; Kandasamy, P.; Kel'in, A. V.; Milstein, S.; Taneja, N.; O'Shea, J.; Shaikh, S.; Zhang, L.; van der Sluis, R. J.; Jung, M. E.; Akinc, A.; Hutabarat, R.; Kuchimanchi, S.; Fitzgerald, K.; Zimmermann, T.; van Berkel, T. J. C.; Maier, M. A.; Rajeev, K. G.; Manoharan, M. *J. Am. Chem. Soc.* **2014**, *136*, 16958.

(7) http://ir.arrowheadresearch.com/eventdetail.cfm?eventid=151555.

(8) Yang, W. *Q. Rev. Biophys.* **2011**, *44*, 1.

(9) Wickstrom, E. *Adv. Drug Delivery Rev.* **2015**, *87*, 25.

(10) Eckstein, F. *Nucleic Acid Ther.* **2014**, *24*, 374.

(11) Wu, S. Y.; Yang, X.; Gharpure, K. M.; Hatakeyama, H.; Egli, M.; McGuire, M. H.; Nagaraja, A. S.; Miyake, T. M.; Rupaimoole, R.; Pecot, C. V.; Taylor, M.; Pradeep, S.; Sierant, M.; Rodriguez-Aguayo, C.; Choi, H. J.; Previs, R. A.; Armaiz-Pena, G. N.; Huang, L.; Martinez, C.; Hassell, T.; Ivan, C.; Sehgal, V.; Singhania, R.; Han, H.-D.; Su, C.; Kim, J. H.; Dalton, H. J.; Kovvali, C.; Keyomarsi, K.; McMillan, N. A. J.; Overwijk, W. W.; Liu, J.; Lee, J.-S.; Baggerly, K. A.; Lopez-Berestein, G.; Ram, P. T.; Nawrot, B.; Sood, A. K. *Nat. Commun.* **2014**, *5*, 3459.

(12) Miller, P. S. *Bio/Technology* **1991**, *9*, 358.

(13) Pav, O.; Kosiova, I.; Barvik, I.; Pohl, R.; Budesinsky, M.; Rosenberg, I. *Org. Biomol. Chem.* **2011**, *9*, 6120.

(14) Doddridge, Z. A.; Bertram, R. D.; Hayes, C. J.; Soultanas, P. *Biochemistry* **2003**, *42*, 3239.

(15) Meade, B. R.; Gogoi, K.; Hamil, A. S.; Palm-Apergi, C.; Berg, A. v. d.; Hagopian, J. C.; Springer, A. D.; Eguchi, A.; Kacsinta, A. D.; Dowdy, C. F.; Presente, A.; Lonn, P.; Kaulich, M.; Yoshioka, N.; Gros, E.; Cui, X.-S.; Dowdy, S. F. *Nat. Biotechnol.* **2014**, *32*, 1256.

(16) Summers, J. S.; Shaw, B. *Curr. Med. Chem.* **2001**, *8*, 1147.

(17) Gryaznov, S. M. *Chem. Biodiversity* **2010**, *7*, 477.

(18) Devi, G. In *Gene Therapy of Cancer*; Walther, W., Stein, U. S., Eds.; Humana Press: New York, 2009; Vol. *542*, p 351.

(19) Mutisya, D.; Selvam, C.; Lunstad, B. D.; Pallan, P. S.; Haas, A.; Leake, D.; Egli, M.; Rozners, E. *Nucleic Acids Res.* **2014**, *42*, 6542.

(20) Kutterer, K. M. K.; Just, G. *Bioorg. Med. Chem. Lett.* **1994**, *4*, 435.

(21) Jones, A. S. *Int. J. Biol. Macromol.* **1979**, *1*, 194.

(22) Kolarovic, A.; Schweizer, E.; Greene, E.; Gironda, M.; Pallan, P. S.; Egli, M.; Rozners, E. *J. Am. Chem. Soc.* **2009**, *131*, 14932.

(23) Isobe, H.; Fujino, T. *Chem. Record* **2014**, *14*, 41.

(24) Geary, R. S.; Norris, D.; Yu, R.; Bennett, C. F. *Adv. Drug Delivery Rev.* **2015**, *87*, 46.

(25) Harborth, J.; Elbashir, S. M.; Vandenburgh, K.; Manninga, H.; Scaringe, S. A.; Weber, K.; Tuschl, T. *Antisense Nucleic Acid Drug Dev.* **2003**, *13*, 83.

(26) Shen, W.; Liang, X.-h.; Sun, H.; Crooke, S. T. *Nucleic Acids Res.* **2015**, *43*, 4569.

(27) Vorbruggen, H.; Ruh-Pohlenz, C. *Org. React.* **1999**, *55*, 1.

(28) Beigelman, L.; Blatt, L.; Wang, G. *PCT Int. Appl.* WO2010108140, 2010.

(29) Beigelman, L.; Blatt, L.; Wang, G.; Rajwanshi, V. K.; Dyatkina, N.; Smith, D. B. *U.S. Pat. Appl. Publ.* US 20120070411, 2012.

(30) Mikhailov, S. N. *Nucleosides Nucleotides* **1988**, *7*, 679.

(31) Mikhailov, S. N.; Meshkov, S. V.; Kuznetsov, D. A.; Lysov, Y. P.; Gorelik, E. S.; Fomicheva, M. V.; Beigel'man, L. N.; Padyukova, N. S. *Bioorg. Khim.* **1989**, *15*, 969.

(32) Wang, G.; Middleton, P. J. *Tetrahedron Lett.* **1996**, *37*, 2739.

(33) Saha, A. K.; Waychunas, C.; Caulfield, T. J.; Upson, D. A.; Hobbs, C.; Yawman, A. M. *J. Org. Chem.* **1995**, *60*, 788.

(34) Østergaard, M. E.; Gerland, B.; Escudier, J.-M.; Swayze, E. E.; Seth, P. P. *ACS Chem. Biol.* **2014**, *9*, 1975.

(35) Beigelman, L.; Karpeisky, A.; Usman, N. *Nucleosides, Nucleotides Nucleic Acids* **1995**, *14*, 901.

(36) Gore, K. R.; Harikrishna, S.; Pradeepkumar, P. I. *J. Org. Chem.* **2013**, *78*, 9956.

(37) Liboska, R.; Snasel, J.; Barvik, I.; Budesinsky, M.; Pohl, R.; Tocik, Z.; Pav, O.; Rejman, D.; Novak, P.; Rosenberg, I. *Org. Biomol. Chem.* **2011**, *9*, 8261.

(38) Martinez-Montero, S.; Deleavey, G. F.; Kulkarni, A.; Martin-Pintado, N.; Lindovska, P.; Thomson, M.; Gonzalez, C.; Gotte, M.; Damha, M. J. *J. Org. Chem.* **2014**, *79*, 5627.

(39) Prakash, T. P.; Lima, W. F.; Murray, H. M.; Li, W.; Kinberger, G. A.; Chappell, A. E.; Gaus, H.; Seth, P. P.; Bhat, B.; Crooke, S. T.; Swayze, E. E. *Nucleic Acids Res.* **2015**, *43*, 2993.

(40) Manoharan, M.; Akinc, A.; Pandey, R. K.; Qin, J.; Hadwiger, P.; John, M.; Mills, K.; Charisse, K.; Maier, M. A.; Nechev, L.; Greene, E. M.; Pallan, P. S.; Rozners, E.; Rajeev, K. G.; Egli, M. *Angew. Chem., Int. Ed.* **2011**, *50*, 2284.

DOI: 10.1021/acs.joc.5b02375
J. Org. Chem. 2016, 81, 2261−2279

(41) Ciuffreda, P.; Loseto, A.; Santaniello, E. *Tetrahedron: Asymmetry* **2004**, *15*, 203.
(42) Ciuffreda, P.; Loseto, A.; Santaniello, E. *Tetrahedron: Asymmetry* **2002**, *13*, 239.
(43) Howgate, P.; Hampton, A. *Carbohydr. Res.* **1972**, *21*, 309.
(44) Ranganathan, R.; Jones, G. H.; Moffatt, J. G. *J. Org. Chem.* **1974**, *39*, 290.
(45) Marx, A.; Erdmann, P.; Senn, M.; Koerner, S.; Jungo, T.; Petretta, M.; Imwinkelried, P.; Dussy, A.; Kulicke, K. J.; et al. *Helv. Chim. Acta* **1996**, *79*, 1980.
(46) De Mesmaeker, A.; Lebreton, J.; Jouanno, C.; Fritsch, V.; Wolf, R. M.; Wendeborn, S. *Synlett* **1997**, *1997*, 1287.
(47) Billich, A.; Stockhove, U.; Witze, H. *Nucleic Acids Res.* **1983**, *11*, 7611.
(48) Karpeiskii, M. Y.; Mikhailov, S. N. *Bioorg. Khim.* **1979**, *5*, 895.
(49) Padyukova, N. S.; Fomicheva, M. V.; Mikhailov, S. N.; Janta-Lipinski, M. *Bioorg. Khim.* **1990**, *16*, 668.
(50) Bligh, C. M.; Anzalone, L.; Jung, Y. C.; Zhang, Y.; Nugent, W. A. *J. Org. Chem.* **2014**, *79*, 3238.
(51) Sorensen, A. M.; Nielsen, P. *Org. Lett.* **2000**, *2*, 4217.
(52) Halligan, K.; Nair, V. *ARKIVOC* **2006**, 101.
(53) Eppacher, S.; Bhardwaj, P. K.; Bernet, B.; Gala, J. L. B.; Knoepfel, T.; Vasella, A. *Helv. Chim. Acta* **2004**, *87*, 2969.
(54) Pradere, U.; Amblard, F.; Coats, S. J.; Schinazi, R. F. *Org. Lett.* **2012**, *14*, 4426.
(55) Legorburu, U.; Reese, C. B.; Song, Q. *Tetrahedron* **1999**, *55*, 5635.
(56) McGee, D. P. C.; Vaughn-Settle, A.; Vargeese, C.; Zhai, Y. *J. Org. Chem.* **1996**, *61*, 781.
(57) Dzhavadova, G. M.; Gurskaya, G. V.; Padyukova, N. S.; Mikhailov, S. N. *Bioorg. Khim.* **1989**, *15*, 976.
(58) Altona, C.; Sundaralingam, M. *J. Am. Chem. Soc.* **1972**, *94*, 8205.
(59) Altona, C.; Sundaralingam, M. *J. Am. Chem. Soc.* **1973**, *95*, 2333.
(60) Davies, D. B.; Danyluk, S. S. *Biochemistry* **1974**, *13*, 4417.
(61) Young, D. W.; Tollin, P.; Wilson, H. R. *Acta Crystallogr., Sect. B: Struct. Crystallogr. Cryst. Chem.* **1969**, *25*, 1423.
(62) Seth, P. P.; Allerson, C. R.; Siwkowski, A.; Vasquez, G.; Berdeja, A.; Migawa, M. T.; Gaus, H.; Prakash, T. P.; Bhat, B.; Swayze, E. E. *J. Med. Chem.* **2010**, *53*, 8309.
(63) Freier, S. M.; Altmann, K.-H. *Nucleic Acids Res.* **1997**, *25*, 4429.
(64) Pallan, P. S.; Yu, J.; Allerson, C. R.; Swayze, E. E.; Seth, P.; Egli, M. *Biochemistry* **2012**, *51*, 7.
(65) Cummins, L. L.; Owens, S. R.; Risen, L. M.; Lesnik, E. A.; Freier, S. M.; McGee, D.; Guinosso, C. J.; Cook, P. D. *Nucleic Acids Res.* **1995**, *23*, 2019.
(66) Egli, M.; Tereshko, V.; Teplova, M.; Minasov, G.; Joachimiak, A.; Sanishvili, R.; Weeks, C. M.; Miller, R.; Maier, M. A.; An, H.; Dan Cook, P.; Manoharan, M. *Biopolymers* **2000**, *48*, 234.
(67) Beese, L. S.; Steitz, T. A. *EMBO J.* **1991**, *10*, 25.
(68) Murray, J. B.; Terwey, D. P.; Maloney, L.; Karpeisky, A.; Usman, N.; Beigelman, L.; Scott, W. G. *Cell* **1998**, *92*, 665.
(69) Brautigam, C. A.; Steitz, T. A. *J. Mol. Biol.* **1998**, *277*, 363.
(70) Brautigam, C. A.; Sun, S.; Piccirilli, J. A.; Steitz, T. A. *Biochemistry* **1999**, *38*, 696.
(71) Pallan, P. S.; Allerson, C. R.; Berdeja, A.; Seth, P. P.; Swayze, E. E.; Prakash, T. P.; Egli, M. *Chem. Commun.* **2012**, *48*, 8195.
(72) Teplova, M.; Wallace, S. T.; Tereshko, V.; Minasov, G.; Symons, A. M.; Cook, P. D.; Manoharan, M.; Egli, M. *Proc. Natl. Acad. Sci. U. S. A.* **1999**, *96*, 14240.
(73) Pettersen, E. F.; Goddard, T. D.; Huang, C. C.; Couch, G. S.; Greenblatt, D. M.; Meng, E. C.; Ferrin, T. E. *J. Comput. Chem.* **2004**, *25*, 1605.
(74) O-Yang, C.; Wu, H. Y.; Fraser-Smith, E. B.; Walker, K. A. M. *Tetrahedron Lett.* **1992**, *33*, 37.
(75) Wang, G.; Smith, D. B.; Beigelman, L.; Deval, J.; Prhavc, M. *U.S. Pat. Appl. Publ.* US20130165400, 2013.
(76) Manoharan, M.; Lackey, J.; Rajeev, K. G.; Zlatev, I. *PCT Int. Appl.* WO2011133868, 2011.
(77) Wang, G.; Deval, J.; Hong, J.; Dyatkina, N.; Prhavc, M.; Taylor, J.; Fung, A.; Jin, Z.; Stevens, S. K.; Serebryany, V.; Liu, J.; Zhang, Q.; Tam, Y.; Chanda, S. M.; Smith, D. B.; Symons, J. A.; Blatt, L. M.; Beigelman, L. *J. Med. Chem.* **2015**, *58*, 1862.
(78) Kachare, D.; Song, X.-P.; Herdewijn, P. *Bioorg. Med. Chem. Lett.* **2014**, *24*, 2720.
(79) Seamon, K. J.; Hansen, E. C.; Kadina, A. P.; Kashemirov, B. A.; McKenna, C. E.; Bumpus, N. N.; Stivers, J. T. *J. Am. Chem. Soc.* **2014**, *136*, 9822.
(80) Chidgeavadze, Z. G.; Beabealashvilli, R. S.; Padyukova, N. S.; Mikhailov, S. N. *Bioorg. Khim.* **1991**, *17*, 678.

DOI: 10.1021/acs.joc.5b02375
J. Org. Chem. 2016, 81, 2261−2279